R-1838

ORNL-TM-5011

Irradiation Performance of HTGR Fuel Rods in HFIR Experiment HRB-6

F. J. Homan
E. L. Long, Jr.
B. H. Montgomery
R. L. Hamner
K. H. Valentine

OAK RIDGE NATIONAL LABORATORY
OPERATED BY UNION CARBIDE CORPORATION • FOR THE U S ATOMIC ENERGY COMMISSION

BLANK PAGE

Printed in the United States of America. Available from
National Technical Information Service
U.S. Department of Commerce
5285 Port Royal Road, Springfield, Virginia 22161
Price: Printed Copy $5.45; Microfiche $2.25

ORNL-TM-5011
(UC-77 Gas-Cooled
Reactor Technology)

Contract No. W-7405-eng-26

METALS AND CERAMICS DIVISION

IRRADIATION PERFORMANCE OF HTGR FUEL RODS IN HFIR EXPERIMENT HRB-6

F. J. Homan, E. L. Long, Jr., B. H. Montgomery,
R. L. Hamner, and K. H. Valentine

DECEMBER 1975

OAK RIDGE NATIONAL LABORATORY
Oak Ridge, Tennessee 37830
operated by
UNION CARBIDE CORPORATION
for the
U.S. ENERGY RESEARCH AND DEVELOPMENT ADMINISTRATION

CONTENTS

IRRADIATION PERFORMANCE OF HTGR FUEL RODS IN HFIR EXPERIMENT HRB-6

F. J. Homan, E. L. Long, Jr., B. H. Montgomery,
R. L. Hamner, and K. H. Valentine

ABSTRACT

The HRB-6 Capsule was irradiated in the RB-5 facility of the High Flux Isotope Reactor (HFIR) for eight cycles. The experiment was in the reactor from February 1973 through September 1973. The primary purpose of this experiment was to test the then reference recycle fissile fuel — Bisco coated mixed thorium-uranium oxide. Among the several secondary objectives was to determine whether there was any difference in irradiation performance of ^{233}U and ^{235}U. Experiment HRB-6 was the first test of fully enriched (93%) ^{235}U in HFIR tests. Both slug injection and extrusion fabrication techniques were used to prepare specimens for this test.

No detectable difference between ^{233}U and ^{235}U irradiation performance could be seen from this experiment. The migration rates for the mixed oxide kernels measured for the HRB-6 specimens were consistent with such measurements made on similar kernels in other experiments. Analysis of the entire body of data on thermal migration for mixed oxide fissile kernels later led to the conclusion that this fuel was a marginal performer, and ultimately was replaced as the reference fuel by an uranium oxycarbide fissile kernel loaded from ion exchange resins. The observation of identical performance for ^{233}U and ^{235}U in the mixed oxide system was very important to the fuel development program. The recycle fuel development efforts have continued to use ^{235}U in subsequent irradiation tests, at considerably less expense than if ^{233}U test specimens were used. The very good performance of the test specimens fabricated using extrusion, relative to those fabricated using slug injection, was noted again in HRB-6.

INTRODUCTION

The HRB-6 experiment was the sixth in a series of HTGR fuel irradiations conducted in the removable beryllium (RB) facility of the High Flux Isotope Reactor (HFIR). As with the five previous experiments

in this series,[1-4] fuel specimens in the HRB-6 capsule were predominantly rods containing closely packed coated particles. The particles contained thorium as the fertile material and a thorium-uranium mixed oxide as the fissile particle. All of the fertile particles were a Biso design, consisting of a kernel, a porous buffer layer of pyrolytic carbon, followed by a dense layer of pyrolytic carbon. Some of the fissile particles were a Biso design, and some were Triso. The Triso design consists of kernel, buffer, dense PyC, SiC, and another layer of dense PyC. The coated particles were formed into fuel rods by bonding the particles together with a carbonaceous binder material.

The objectives of the HRB-6 experiment were:

1. to compare the irradiation behavior of Biso coated 4:1 (Th,^{233}U)O_2 with Biso coated 4:1 (Th,^{235}U)O_2 as loose particles and in bonded fuel rods,
2. to supply samples of particles containing ^{233}U and ^{235}U for study of fission product retention within the coated particles and within a carbonaceous matrix,
3. to determine whether the differing fission product spectra from ^{233}U and ^{235}U affect the carbon transport and kernel migration within coated particles,
4. to test further fueled specimens prepared by extrusion, slug-injection, and intrusion bonding for dimensional stability when irradiated to full HTGR fluence,
5. to continue testing ultrasonic thermometers for measuring center-line temperature of the fuel.

The HRB-6 capsule contained 13 fuel specimens, two were fabricated by extrusion, one by hot-intrusion, and the remainder by slug injection. The extruded and hot-intrusion specimens contained a central hole to accommodate an ultrasonic thermometer, which measured the center line temperature of hot intrusion specimen 1C. Six of the 13 specimens (2A, 2B, 2C, 4A, 4B, and 4C) were fabricated by the General Atomic Company (GAC). These specimens were returned to GAC for postirradiation examination. Because these specimens were fabricated and examined at GAC, very little will be said about them in this report.

---

[1] J. L. Scott et al., *An Irradiation Test of Bonded HTGR Coated Particle Fuels in an Instrumented Capsule in HFIR*, ORNL-TM-3640 (March 1972).

[2] J. H. Coobs et al., *Irradiation Performance in HFIR Experiment HRB-2 of HTGR Fuel Sticks Bonded with Reference and Advanced Matrix Materials*, ORNL-TM-3988 (January 1973).

[3] F. J. Homan et al., *Irradiation Performance of HTGR Fuel Rods in HFIR Experiment HRB-3 and ETR Experiment P13N*, ORNL-TM-4526 (October 1974).

[4] F. J. Homan et al., *Irradiation Performance of HTGR Fuel Rods in HFIR Experiments HRB-4, -5*, report in preparation.

DESCRIPTION OF HRB-6 CAPSULE AND FUEL SPECIMENS

Capsule

Capsule HRB-6 was similar in design to the previous five capsules in this series.[1-4] Thirteen fuel specimens having a total stack length of 15.33 in. were supported in a one-piece sleeve made of Poco graphite, grade AXF-5Q. The graphite sleeve was contained inside a double-walled water-cooled stainless steel vessel 1.292-in. OD and 0.963 in. ID. A cross section of HRB-6 is shown in Fig. 1.

The capsule was designed to obtain reasonably uniform axial temperatures by tapering the graphite sleeve so as to increase the gas gap between the graphite and the stainless steel wall. This taper varies the thermal resistance between the graphite and the capsule wall to compensate for the lower neutron fluxes at the ends of the capsule. To compensate for the overall power variations with time, the composition of the helium-neon sweep gas mixture that fills the gap between the fuel and the graphite, and the gap between the graphite and the stainless steel wall, was varied to maintain the peak fuel temperature at the design value.

Nominal dimensions of the fuel and graphite sleeve are given in Fig. 2. The exact dimensions of the sleeve are shown in Fig. 3. Figure 3 also contains the postirradiation dimensional changes, and bow of the sleeve, which will be discussed in more detail in the section on thermal analysis in Appendix A.

Temperatures inside the capsule were monitored by nine Chromel-Alumel thermocouples. These thermocouples were sheathed in 0.0625-in.-diam stainless steel tubing, and the sheathed couples were coated with a 0.0025-in.-thick protective barrier of copper. These thermocouples were located in axial holes in the graphite sleeve adjacent to the fuel specimens as shown in Figs. 2 and 4. The ultrasonic thermometer was located at the center line of specimen 1C. Specimens 1A, 1B, and 1C were all hollow to accommodate the positioning of this thermometer.

Fuel

Loading Scheme

The 13 specimens irradiated in HRB-6 were loaded as shown in Fig. 2. Specimens 1A and 1B were extrusions and specimen 1C was a fueled bonded bed[5] prepared by intrusion bonding. Specimen 1C contained six Poco graphite holders for loose coated particles. The remainder of the specimens were formed by slug injection. Specimens 2A, 2B, 2C, 4A, 4B, and 4C were fabricated at General Atomic Company and will not be described in this report. The heavy metal loadings for the seven ORNL specimens are given in Table 1.

---

[5]The fueled bonded bed was an intrusion bonded fuel rod formed around six tubes containing loose particles.

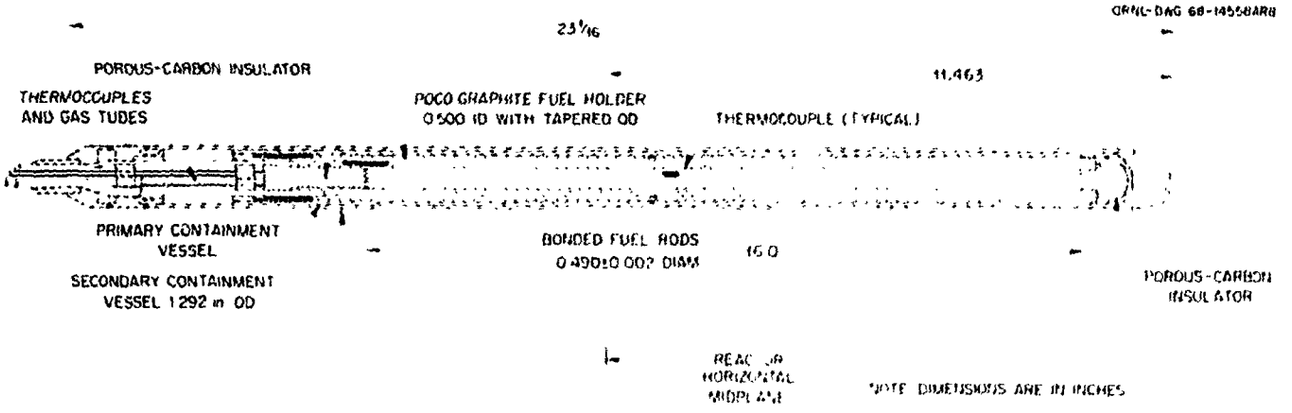

Fig. 1. Cross Section of HTGR Instrumented Capsule HRB-6.

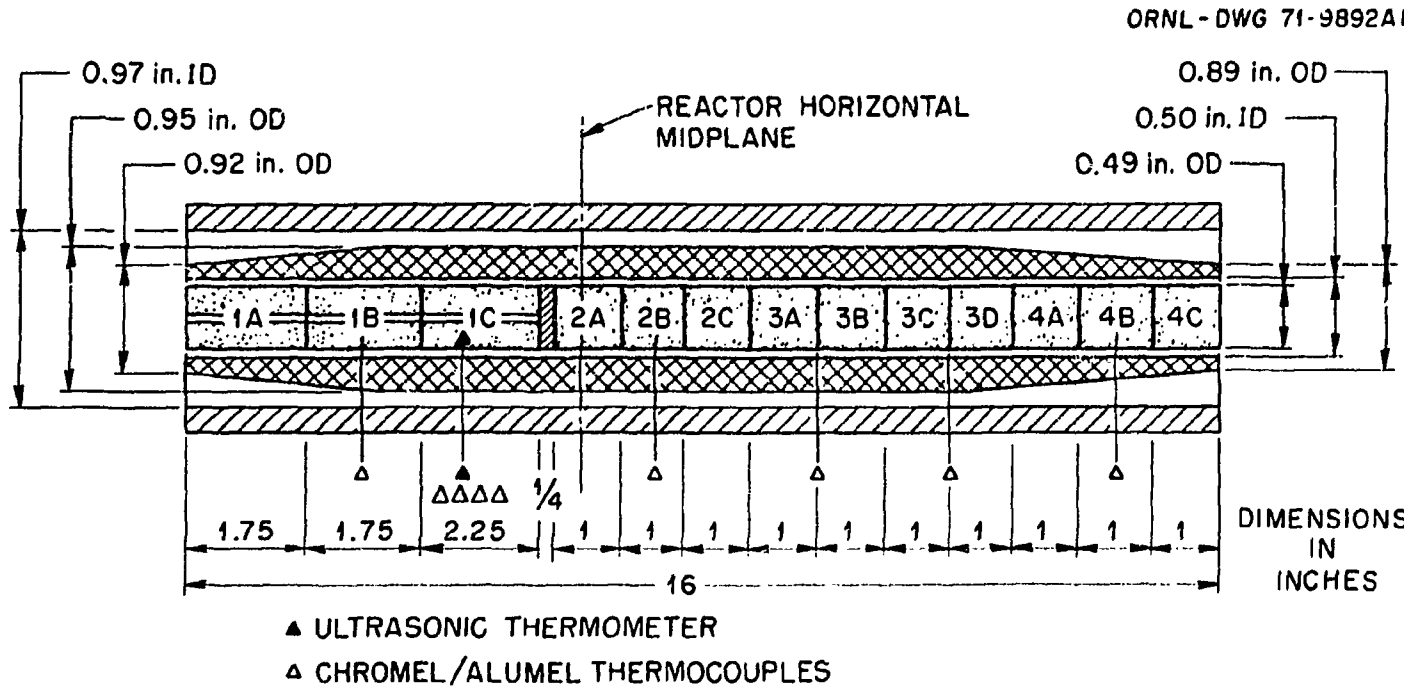

Fig. 2. Experiment HRB-6 Configuration.

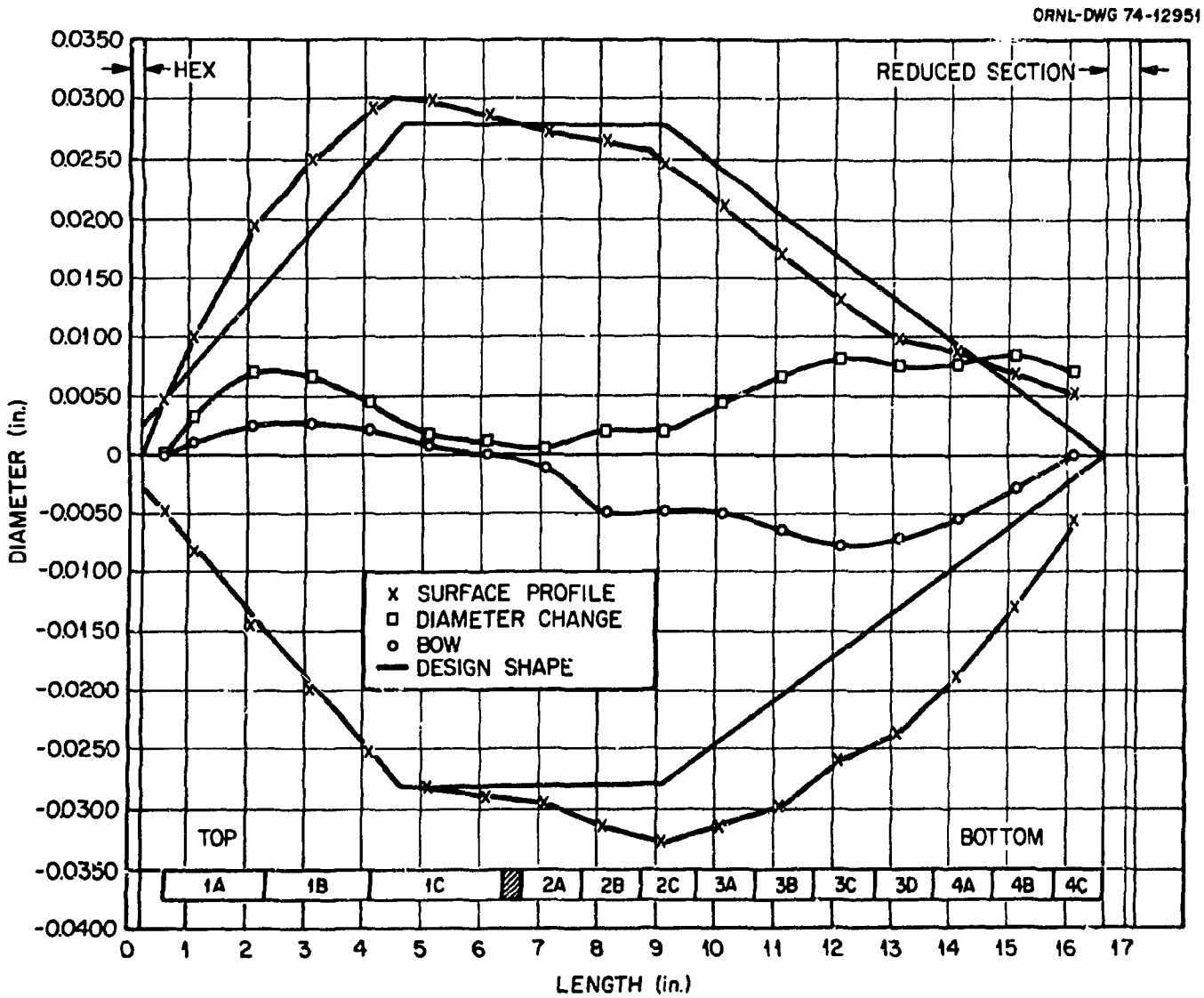

Fig. 3. Graphite Sleeve Dimensions for Capsule HRB-6 0° Orientation.

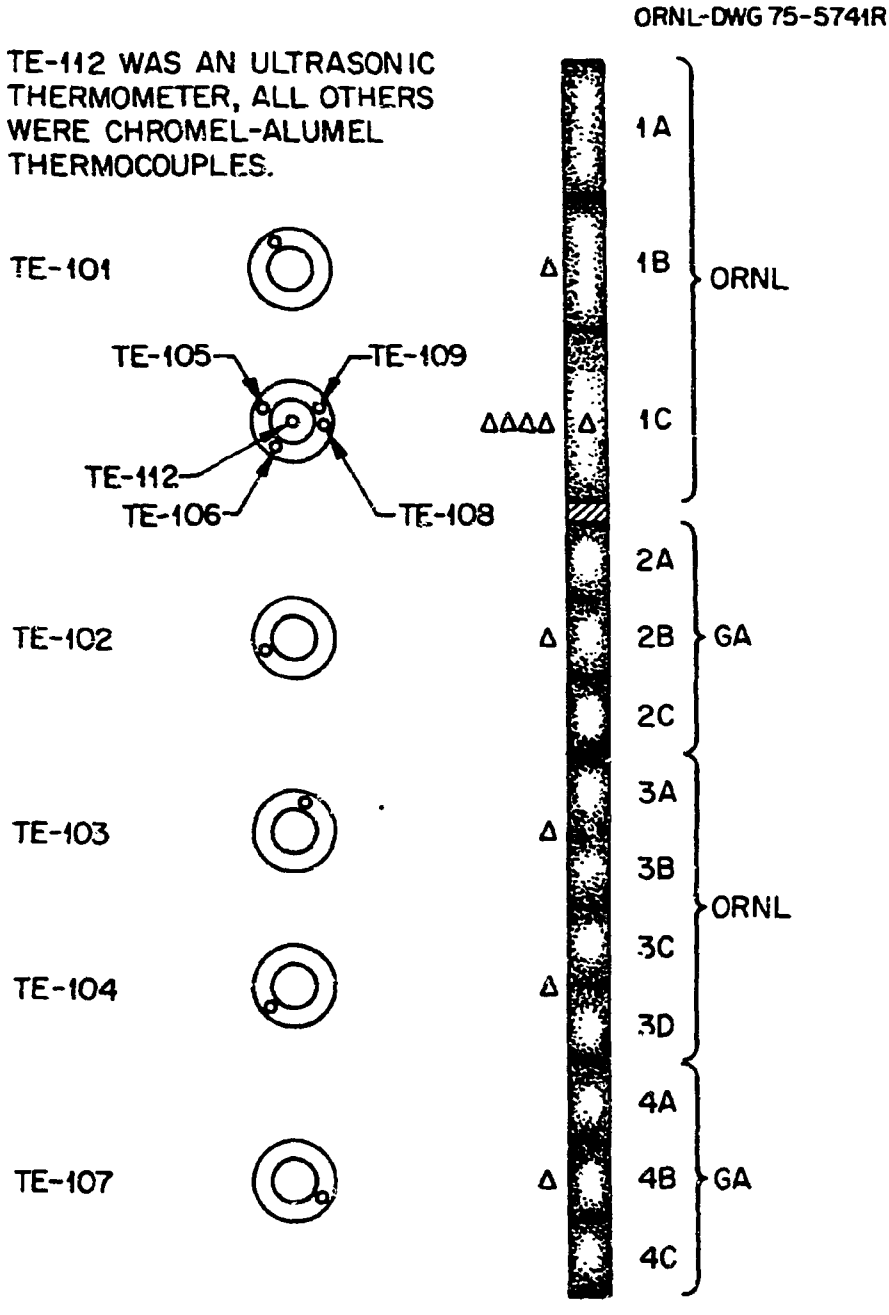

Fig. 4. Experiment HRB-6 Fuel Specimen and Thermocouple Locations.

Table 1. Fuel Loadings for HRB-6

Specimen	Heavy Metal Content, g/cm^3			
	^{233}U	^{235}U	^{238}U	^{232}Th
1A		0.0060	0.0004	0.2540
1B		0.0061	0.0004	0.2626
1C	0.0063[a]		0.0004	0.2680
3A	0.0052		ND[b]	0.2300
3B		0.0050	0.0004	0.2364
3C	0.0052		ND	0.2365
3D		0.0050	0.0004	0.2349

[a]Combined ^{233}U and ^{235}U.

[b]ND = not determined.

Coated Particles

Three types of coated particles were used in the HRB-6 fuel specimens: fertile, fissile, and inert. The fertile kernels were prepared by the sol-gel process (SG). The fissile kernels were prepared by either sol-gel or from weak-acid resins (WAR). The inert kernels were desulfurized carbon derived from strong-acid resin (SAR). The Bisco-coated inert particles were common to all specimens. The Bisco-coated fertile particles, coated by GAC, were common to all specimens except specimen 1C in which a different Bisco coated SG thoria particle was used. The characteristics of all particles are given in Table 2. The types of fissile particles contained in the ORNL fuel specimens are listed in Table 3.

Preparation of Specimens

A general description of the fabrication of ORNL specimens is presented in Table 4. The extrusions were nominally 0.490-in. OD and 1.75 in. long with a 0.090-in. center hole for placement of an ultrasonic thermometer to measure fuel center-line temperature. The components were mixed by hand as a slurry in acetone until the acetone evaporated, extruded at room temperature at a pressure of 1000 psi, cured at 90°C for 16 hr, then carbonized at 1000°C on a 24-hr cycle. Metallographic examination revealed that there was axial cracking in the matrix and in specimen type 1B, some cracked coatings on fertile and inert particles after heat treatment at 1800°C. The matrix cracking was attributed to the high volume loadings (43 and 44 vol % for 1A and 1B, respectively), which tended to restrain the matrix as it shrunk during

Table 2. Characterization of Coated Particles for HRB-6

Coated Particle									
Batch Number	OR-1909	OR-1910	6542-06-011[a]	OR-1562	OR-1892, -1900	Pu-291	Pu-295b	Pu-296	Pu-297
Type Kernel Material[b]	$(4Th,U)O_2$	$(4Th,U)O_2$	ThO_2	ThO_2	Carbon[c]	$(4Th,U)O_2$	UO_2-UC_2[f]	UC_2[f]	$UC_2 + C$[f]
Uranium Content, wt %	8.22	7.29				5.61	29.3	31.4	29.4
^{235}U Enrichment, at. %	93.17	93.17							
^{233}U Enrichment, at. %						97.97	97.97	97.97	97.97
Thorium Content, wt %	32.3	28.3	52.32	51.6		23.81			
				Average (standard deviations)					
Kernel									
Diameter, μm	366 (27.7)	366 (27.7)	504 (7.6)	398.3 (17.1)	448 (31.5)	351 (31.0)	385 (ND)	448 (18)	385 (ND)
Density, g/cm^3	ND[g]	ND	9.99 (ND)	9.9 (ND)	1.2 (ND)	10 (ND)	3.2(ND)	3.8 (ND)	3.7 (ND)
Buffer									
Thickness, μm	97.3 (14.1)	97.7 (12.3)	96 (13.9)	54.7 (8.1)	ND	105 (5.5)	36 (4.2)	30.9 (4.4)	36.1 (5.3)
Density, g/cm^3	1.0[d] (ND)	1.1 (ND)	1.16 (ND)	1.2[d] (ND)	1.0[d] (ND)	1.0[d] (ND)	1.1[d] (ND)	1.0[d] (ND)	1.1[d] (ND)
Inner Carbon Coating									
Thickness, μm		31.0 (1.04)					24.4 (3.3)	26.3 (2.4)	27.9 (3.2)
Density, g/cm^3		ND					1.95[d] (ND)	1.95[d] (ND)	1.95[d] (ND)
SiC									
Thickness, μm		26.8 (1.4)					36.5 (1.6)	30 (1.5)	29.3 (ND)
Density, g/cm^3		3.2 (0.005)					3.19[d] (ND)	3.19[d] (ND)	3.2[d] (ND)
Outer Carbon Coating									
Thickness, μm	93.4 (4.1)	41.4 (3.8)	93 (10.8)	76.2 (6.4)	140.4[e] (ND)	85.0 (6.0)	16 (1.5)	20.2 (2.2)	19.4 (2.0)
Density, g/cm^3	2.05 (0.002)	1.98 (0.005)	1.81 (0.007)	1.97 (0.007)	1.917 (0.0097)	1.98 (0.007)	1.98[d] (ND)	1.98[d] (ND)	1.98[d] (ND)

[a] Coated by GAC.

[b] All kernel material is derived by the SG method unless noted otherwise.

[c] Derived from desulfurized SAR.

[d] Calculated from run conditions.

[e] Buffer- and outer-coating thicknesses measured together.

[f] Derived from WAR.

[g] ND = not determined.

Table 3. Fissile Particles in ORNL Fuels

Specimen	Holder	Type of Coated Fissile Particle	Batch
1A		Triso-coated SG 4:1 (Th,^{235}U)O_2	OR-1910
1B		Biso-coated SG 4:1 (Th,^{235}U)O_2	OR-1909
1C	1	Biso-coated SG 4:1 (Th,^{235}U)O_2	OR-1909
	2	Triso-coated SG 4:1 (Th,^{235}U)O_2	OR-1910
	3	Biso-coated SG 4:1 (Th,^{233}U)O_2	Pu-291
	4	Triso-coated WAR $^{233}UO_2$ + UC_2	Pu-295b
	5	Triso-coated WAR $^{233}UO_2$	Pu-296
	6	Triso-coated WAR $^{233}UC_2$ + C	Pu-297
	Bonded Bed	Triso-coated SG 4:1 (Th,^{235}U)O_2	OR-1910
3A, 3C		Biso-coated SG 4:1 (Th,^{233}U)O_2	Pu-291
3B, 3D		Biso-coated SG 4:1 (Th,^{235}U)O_2	OR-1909

Table 4. General Description of Specimens for HRB-6

Specimen Type	Fabrication Technique	Matrix Filler Material[a]		Carbonization Mode
		(wt %)	Type[b]	
1A 1B	Extrusion	60 19	Graphitized Robinson coke Thermax	In covered graphite tray
1C[c]	Intrusion Bonding	40	RC-4	In bed of graphite powder
3A, 3B 3C, 3D	Slug Injection	38.7	C-4	In bed of alumina powder

[a]Binders used were Varcum for extrusions and Ashland Oil Company A-240 pitch for all other specimens.

[b]Filler material designations and sources are as follows: Isotropic Robinson graphitized coke originally produced for AFML by Union Carbide Corporation; Thermax, carbon black, from R. T. Vanderbilt Company; and Isotropic RC-4 graphite flour from Airco-Speer Corporation.

[c]Fueled bonded bed holder.

carbonization and heat treatment; this restraint along with the strong bonding of the matrix to coated particles probably caused the damage to some coatings.

The loose particles in specimen 1C were carefully sized so they would stack in a single row in the holders as shown in Fig. 5. A precise number of particles were placed in each holder to give a specified fuel loading. Because three of the particle types were relatively small, it was necessary to expand the particle beds uniformly over the length of the holder with larger sized coated ThO_2 particles.

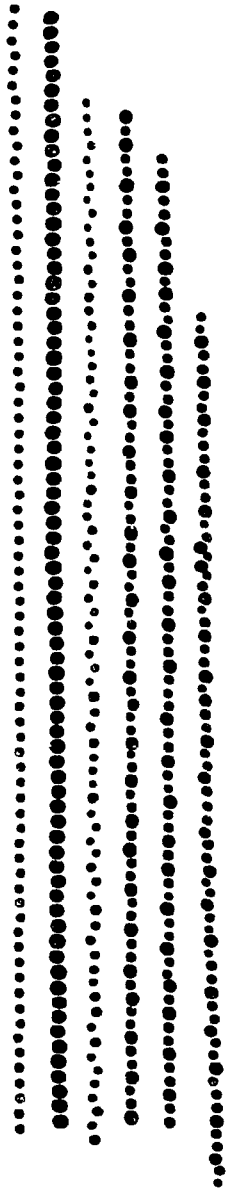

Fig. 5. Radiograph Showing Alignment of Loose Coated Particles in Individual Graphite Holders for Specimen 1C Capsule HRB-6.

The graphite holders were inserted in holes of a fueled bonded bed spaced 60° apart around the central hole. The bonded bed, containing fissile and fertile particles to generate the necessary fission heat, was formed by intrusion bonding in a metal mold around wooden rods. After carbonization the residue from the rods was removed, leaving holes for insertion of the graphite holders.

Specimens 3A, 3B, 3C, and 3D were formed by slug injection to nominal dimensions of 0.490 in. in diameter by 1.0 in. long. The matrix was injected into the fuel beds at a temperature of 175°C and at a pressure of 1000 psi. All were carbonized vertically in a packed bed of alumina at 850°C. Matrix densities for 3A and 3C were higher than those for 3B and 3D and the pitch coke yield was slightly higher. Since rods 3A and 3C were fabricated in a glove box facility and rods 3B and 3D were fabricated in a contact facility, it is suspected that the differences in matrix characteristics resulted from slight differences in carbonization conditions in the two furnaces (heating rate and/or atmosphere purity).

All specimens for the experiment were heat treated at 1800°C to stabilize the matrix, after which they were characterized by photography, radiography, and metallography. Fuel distribution was good in all specimens and dimensions were within the tolerance specified. Data summaries of these characterizations are given in Tables 1 and 5.

Table 5. Physical Characteristics of Specimens for HRB-6

Specimen Number	Specimen	Average Diameter (in.)		Average Length (in.)	Particle Volume Loading (%)	Matrix Density $(g/cm)^3$	Pitch Coke Yield (%)
		Outside	Inside				
JI-74-4	1A	0.4921	0.0925	1.769	42.81	1.50	ND
JI-51-5	1B	0.4907	0.0925	1.756	44.26	1.62	ND
JI-80-2[a]	1C	0.4912	0.0920	2.235	ND[b]	ND	ND
M86A055	3A	0.488		0.997	60.7	0.81	32.1
M86A048	3B	0.490		0.972	61.7	0.76	25.1
M86A057	3C	0.488		0.981	61.6	0.81	32.1
M86A050	3D	0.490		0.980	61.3	0.74	25.1

[a]Data for bonded bed holder.

[b]ND = not determined.

DESCRIPTION OF IRRADIATION

Irradiation Conditions

Capsule HRB-6 was irradiated in the RB-5 facility of the HFIR. The location of this facility was shown in the topical report describing the HRB-3 experiment[6] and will not be shown again here. The neutron fluxes, and gamma heating characteristics of the RB-5 facility were also given.[6]

Capsule Operation

The HRB-6 Capsule was inserted into the HFIR at the beginning of fuel cycle 89 on February 27, 1973. The capsule was operated for eight cycles (183.36 days at 100 MW reactor power) to a peak fast fluence of 7.9×10^{21} n/cm^2 (E >0.18 MeV). The irradiation was completed and the capsule removed on schedule on September 8, 1973. The fission heat rate generation as a function of time is given for each specimen in the capsule in the section of this report covering thermal analysis (Appendix A). The large dip in power during the first two cycles was due to the burnout of the ^{235}U isotope. Unlike HRB-4 and -5 (ref. 7), there was little ^{238}U in the specimens, so although there was sufficient ^{232}Th to eventually produce enough ^{233}U to bring the power level back up, the long decay time for the ^{233}U precursors resulted in a burnup of the initial fissile material before the bred-in ^{233}U appeared in sufficient amounts to maintain power. When significant amounts of ^{238}U are present in the as-fabricated fuel, this problem is partially overcome by the more rapid buildup of ^{239}Pu. The isotopic burnup and fluences for each specimen are presented in Table 6. These calculations were based on a peak fast flux (E >0.18 MeV) of 5×10^{14} n cm^{-2} sec^{-1} and a perturbed thermal flux (E <0.41 eV) of 1.18×10^{15} n cm^{-2} sec^{-1}. Both peak fluxes were assumed at the horizontal midplane (HMP) of the reactor.

Fission gas release-to-birth rate ratios (R/B) as determined from sweep gas samples are shown in Fig. 6. No R/B data were taken until the middle of May, 1973, (approximately 75 days into the irradiation) because of the unusually high fission gas release that appeared at the beginning of the irradiation. The activity was too high for sampling, and it became necessary to cut the sweep gas flow (normally 60 cm^3/min) to a few cubic centimeters per minute. The sweep gas activity decreased with time until after about three cycles it was possible to reinstate normal sweep flow rates and take gas samples. The initial activity release was evidently due to the early failure of highly enriched particles. The release decreased as the fuel in these particles was consumed and power generation switched to the

---

[6] F. J. Homan et al., *Irradiation Performance of HTGR Fuel Rods in HFIR Experiment HRB-3 and ETR Experiment P13N*, ORNL-TM-4526 (October 1974).

[7] F. J. Homan et al., *Irradiation Performance of HTGR Fuel Rods in HFIR Experiments HRB-4, -5*, report in preparation.

Table 6. Experiment HRB-6 Fuel Specimen Burnups, Fluxes, and Fluences

Specimen	Percent Initial Isotope Fissioned[a]		Distance HMP[b] to Specimen Center (in.)	Average Fluxes, n cm^{-2} sec^{-1}		Fluences, n/cm^2	
	^{238}U	^{232}Th		Thermal (E <0.414 eV)	Fast (E >0.18 MeV)	Thermal (E <0.414 eV)	Fast (E >0.18 MeV)
1A	20.2	9.8	5.500	7.49×10^{-14}	3.70×10^{-14}	1.2×10^{-22}	5.8×10^{-21}
1B	23.5	12.3	3.750	9.38	4.35	1.5	6.8
1C	25.9	14.2	1.750	10.88	4.90	1.7	7.7
2A	26.5	15.0	−0.125	11.71	5.00	1.8	7.9
2B	26.5	15.0	−1.125	11.80	4.98	1.8	7.9
2C	25.0	14.3	−2.125	11.68	4.83	1.8	7.6
3A	23.5	13.5	−3.125	11.20	4.56	1.7	7.2
3B	21.5	12.5	−4.125	10.47	4.24	1.6	6.7
3C	19.0	11.5	−5.125	9.56	3.85	1.5	6.1
3D	16.2	9.6	−6.125	8.50	3.43	1.3	5.4
4A	13.5	8.2	−7.125	7.32	2.99	1.1	4.7
4B	10.5	6.5	−8.125	6.14	2.50	0.97	3.9
4C	7.5	4.8	−9.125	4.90	1.97	0.77	3.1

[a] In all cases, the burnup of ^{233}U or ^{235}U was 84%.

[b] Horizontal Midplane.

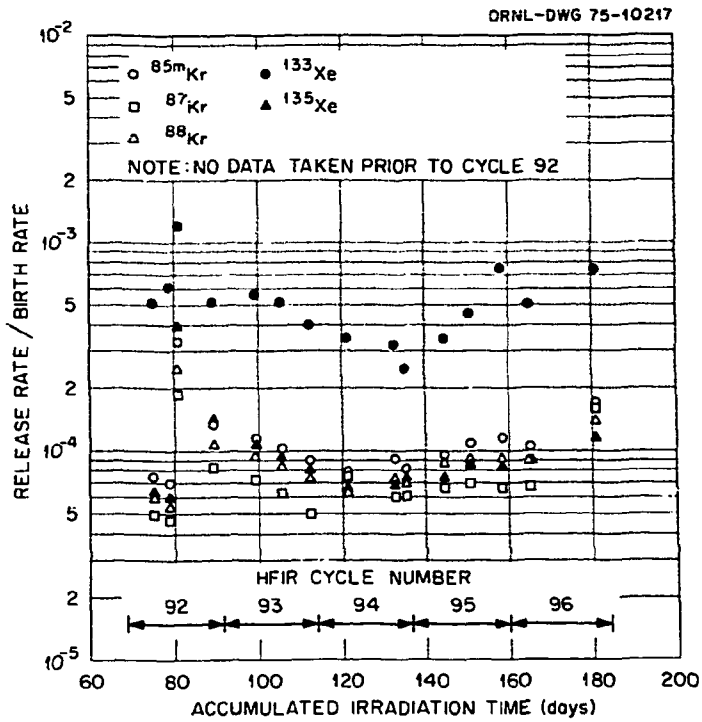

Fig. 6. HFIR HRB-6 Capsule.

thorium containing particles. During this period of high release (February 27 to May 21, 1973), a 100% He sweep gas was used, which resulted in temperatures below design levels. After May 21, neon was added to raise the temperatures.

The operating history of the HFIR during the period capsule HRB-6 was in the reactor is given in Table 7.

Table 7. Experiment HRB-6 Operating History[a]

HFIR Cycle	Cycle Began	Cycle Ended	Time at 100 MW (hr)
89	2/27/73	3/22/73[a]	545.7
90	3/23/73	4/15/73	1094.6
91	4/18/73	5/11/73	1647.5
92	5/11/73	6/3/73	2192.6
93	6/3/73	6/26/73	2738.1
94	6/26/73	7/20/73	3286.2
95	7/22/73	8/15/73	3843.1
96	8/16/73	9/8/73	4400.6

[a]Each cycle was for an irradiation time of 23 days.

Fuel Specimen Temperatures

As described earlier, the HRB-6 capsule temperatures were monitored by nine thermocouples located in the graphite sleeve and an ultrasonic thermometer located at the center line of specimen 1C. The thermal analysis techniques[8] used for the HRB capsules rely heavily on the graphite temperatures as measured with the Chromel-Alumel thermocouples. Therefore, temperatures are computed only for specimens adjacent to the thermocouples. The details of these calculations are rather lengthy and are presented in Appendix A for interested readers. Only the temperature plots for specimens 1B, 1C, 2B, 3A, 3C, 3D, and 4B are shown as Figs. 7 through 14. In these plots, the graphite midwall temperature is shown as the lower plot, the fuel surface temperature is shown as the center plot, and the fuel center temperature is shown as the upper plot. The thermocouples adjacent to specimens 2B and 4B failed prematurely; therefore, the temperatures for these specimens were not calculated for all eight cycles.

---

[8] F. J. Homan, *Thermal Analysis of HTGR Fuel Rods Irradiated in the HFIR Removable Beryllium Facility*, report in preparation.

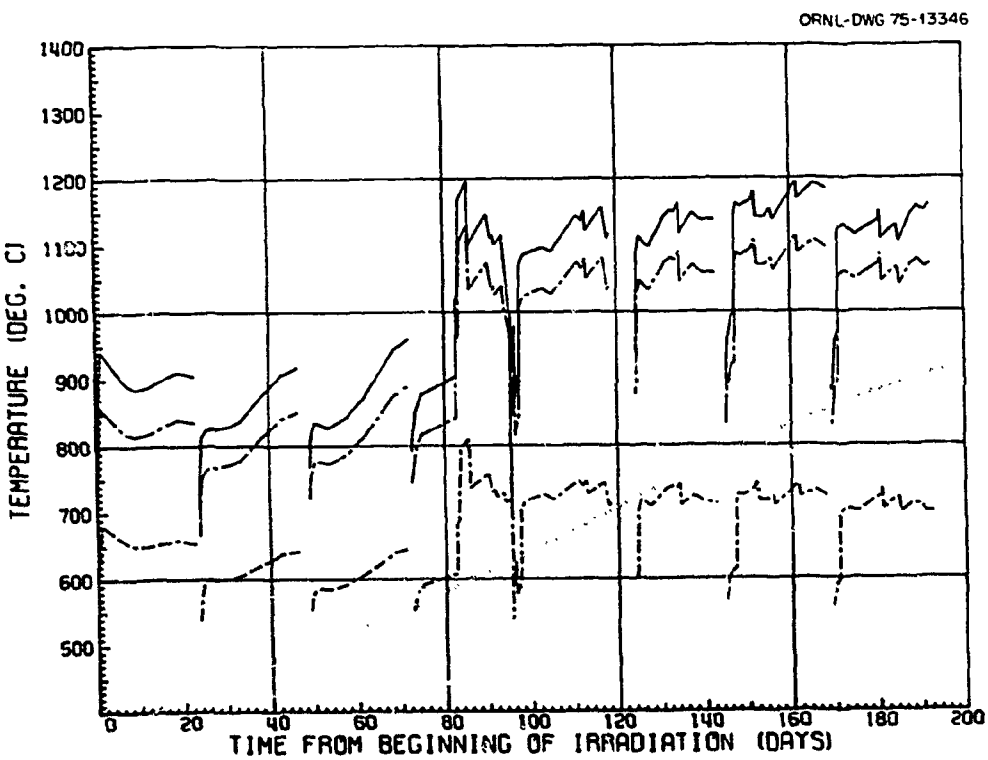

Fig. 7. Graphite Midwall, Fuel Surface, and Fuel Center Temperatures for HRB-6 Specimen 1B.

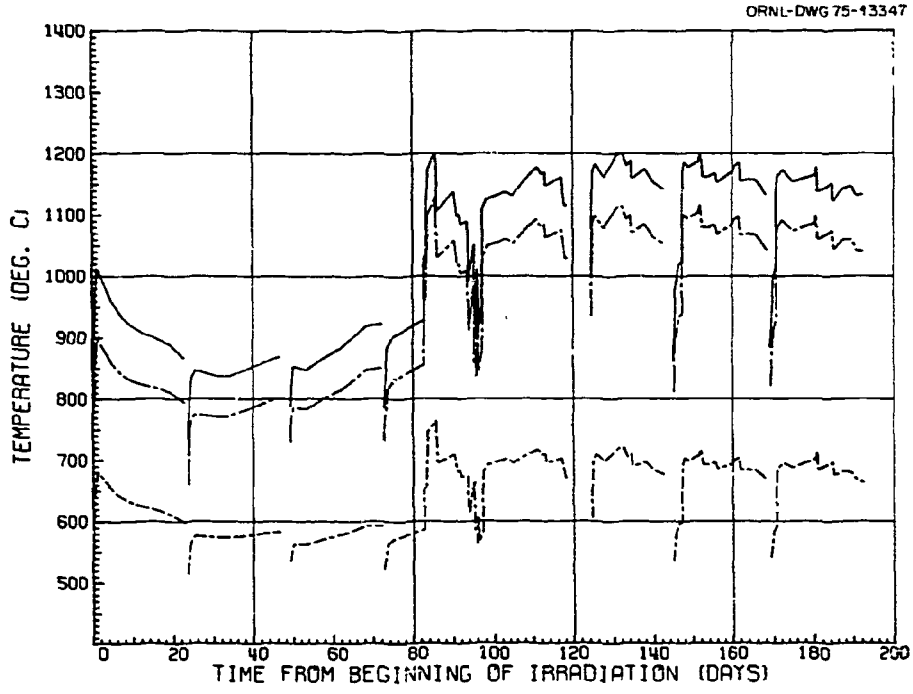

Fig. 8. Graphite Midwall, Fuel Surface, and Fuel Center Temperatures for HRB-6 Specimen 1C.

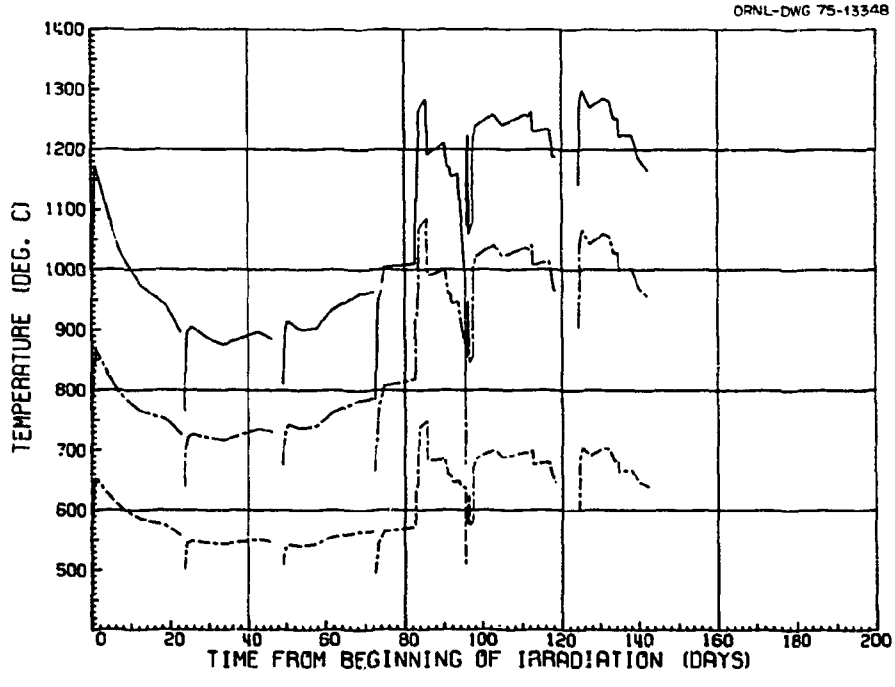

Fig. 9. Graphite Midwall, Fuel Surface, and Fuel Center Temperatures for HRB-6 Specimen 2B.

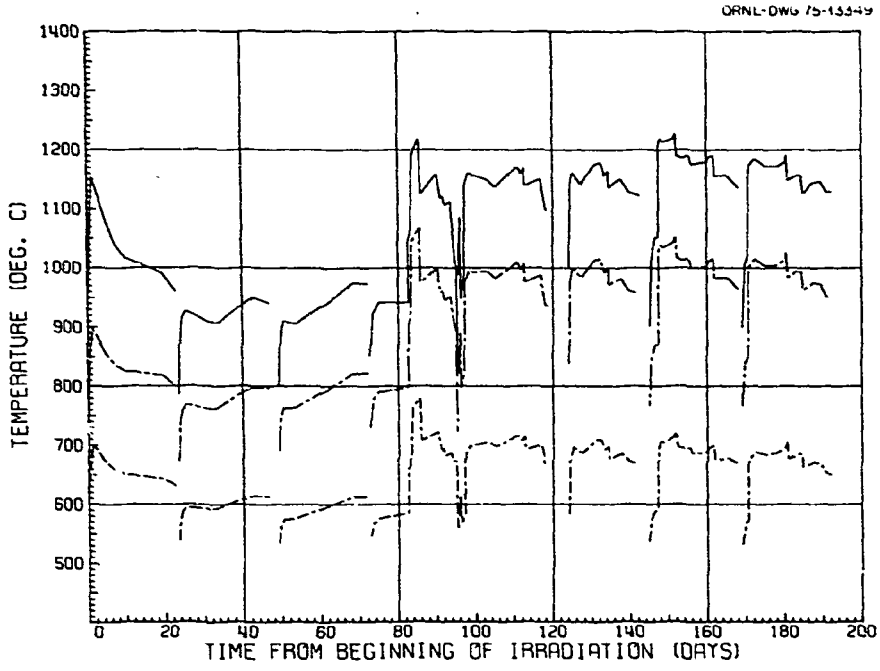

Fig. 10. Graphite Midwall, Fuel Surface, and Fuel Center Temperatures for HRB-6 Specimen 3A.

Fig. 11. Graphite Midwall, Fuel Surface, and Fuel Center Temperatures for HRB-6 Specimen 3B.

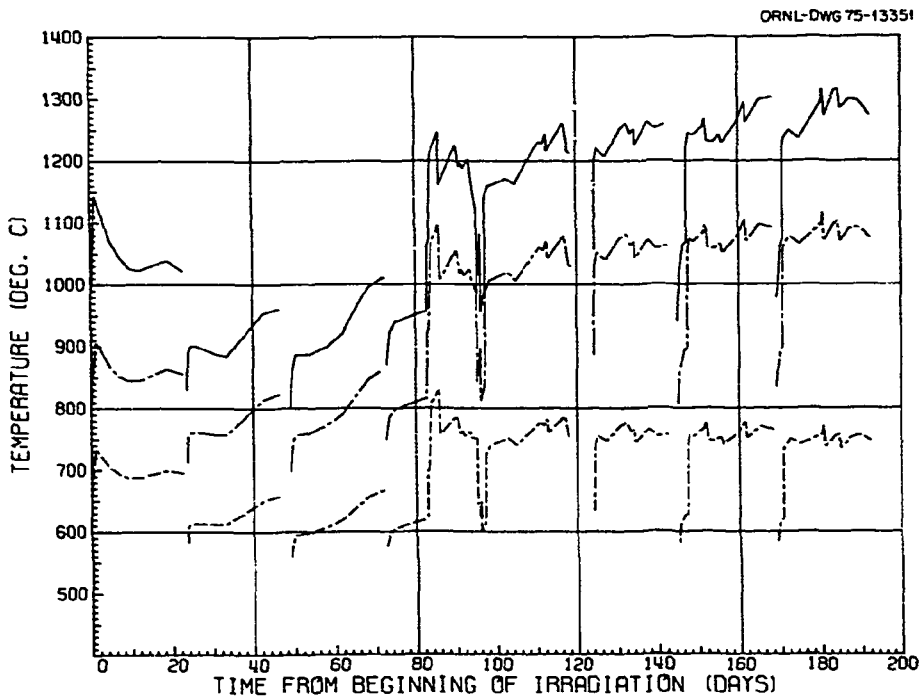

Fig. 12. Graphite Midwall, Fuel Surface, and Fuel Center Temperatures for HRB-6 Specimen 3C.

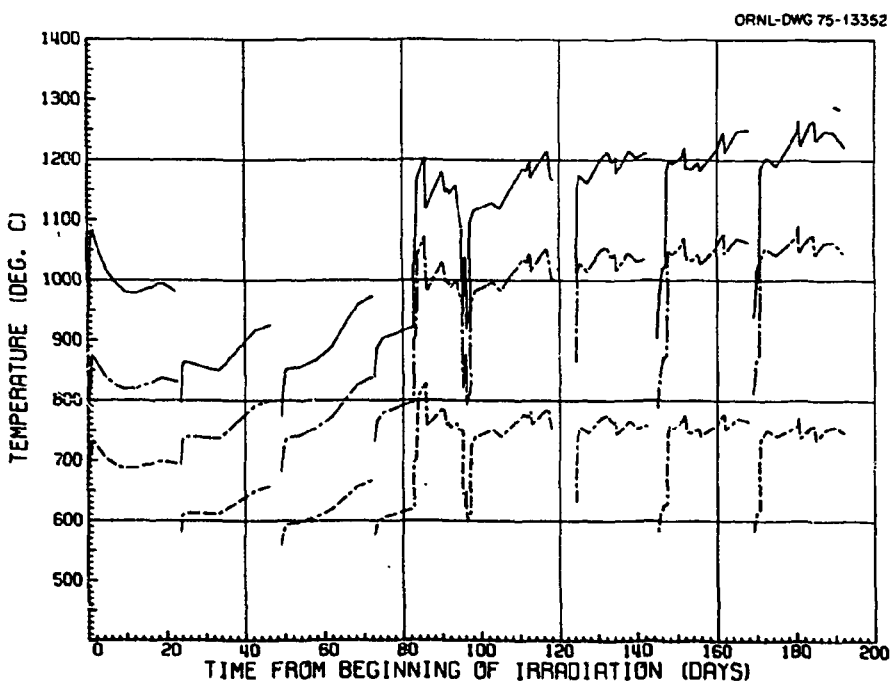

Fig. 13. Graphite Midwall, Fuel Surface, and Fuel Center Temperatures for HRB-6 Specimen 3D.

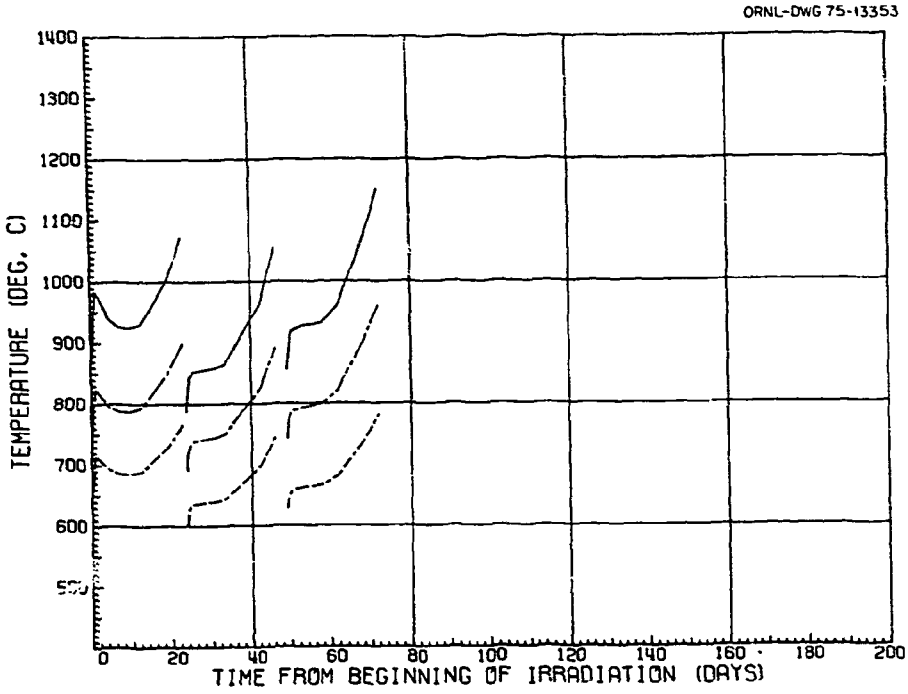

Fig. 14. Graphite Midwall, Fuel Surface, and Fuel Center Temperatures for HRB-6 Specimen 4B.

POSTIRRADIATION EXAMINATION DISASSEMBLY AND VISUAL INSPECTION

The capsule was disassembled by making circumferential cuts through the stainless steel containment vessels above and below the graphite sleeve that contained the fuel rods. After removal of the top and bottom porous graphite plugs, the removal of the fuel rods was attempted by tapping the capsule on the cell floor. The fuel rods were finally removed by pushing them out with a 1/2-in.-diam aluminum rod.

A GAC representative was present during the removal of the fuel and remained to perform the visual examination and to collect dimensional data on their fuel rods. Arrangements were made to ship the GAC fuel rods to their hot cells for additional evaluations.

The general appearance of the extruded fuel rods (1A and 1B) was good with only slight evidence of debonding of the edges (Fig. 15).

The appearance of the slug-injected rods ranged from fair to excellent. Fuel rods 3A and 3C containing ^{233}U fuel, were duplicates, and were fabricated in the glove-box facility. Both fuel rods showed evidence of debonding along their lengths, and their general appearance ranged from fair to good (Fig. 16).

Fuel rods 3B and 3D containing ^{235}U fuel, were duplicates, and were fabricated in contact facility; 3B showed slight evidence of debonding on the ends, and 3D appeared excellent (Fig. 17).

The ORNL rods were intact with the exception of the bonded rod holder 1C, which proved to be very fragile. Rod 1C is shown in Fig. 18

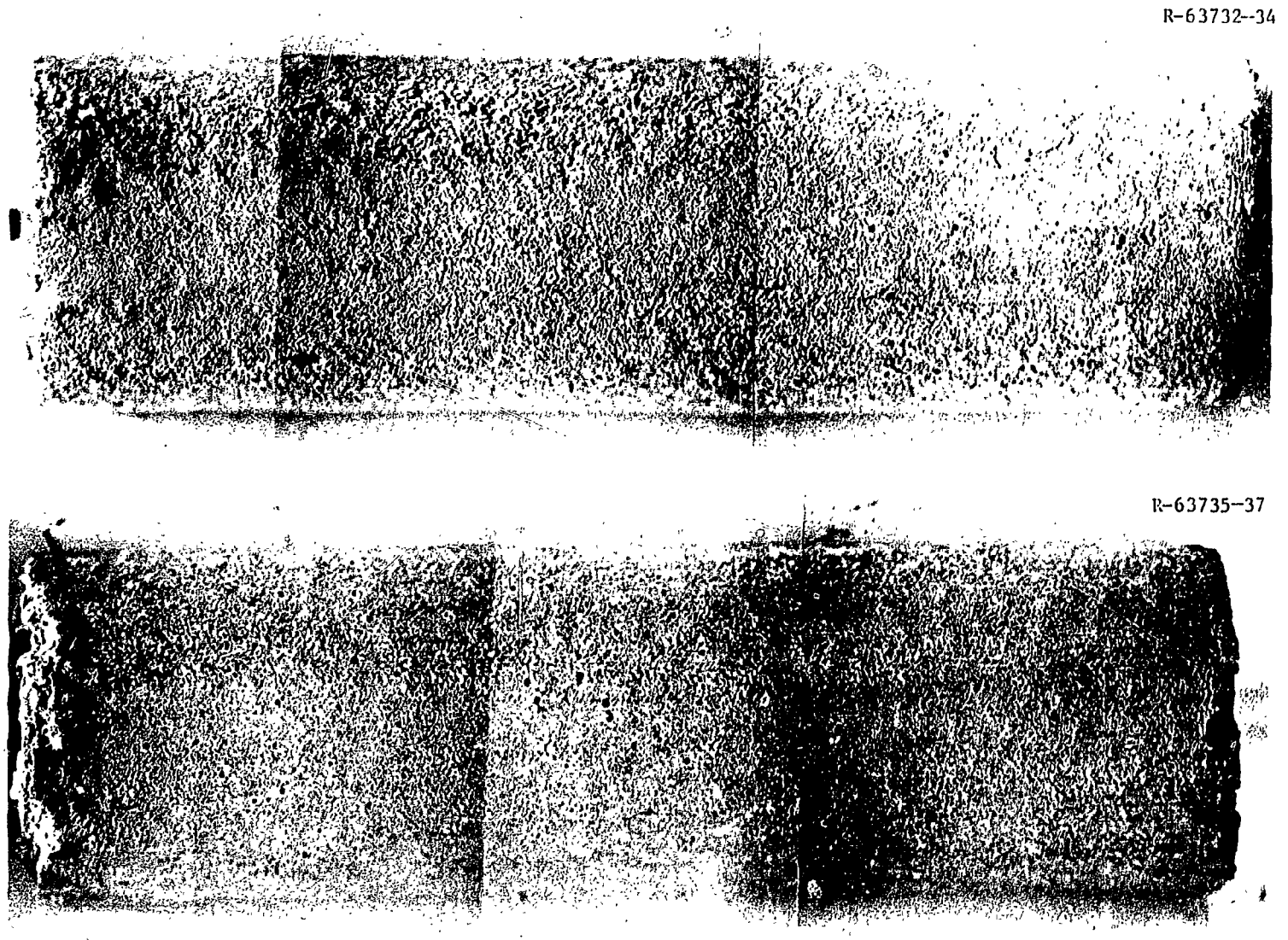

Fig. 15. Extruded Fuel Rods 1A(Top) and 1B Irradiated in Capsule HRB-6. 5×.

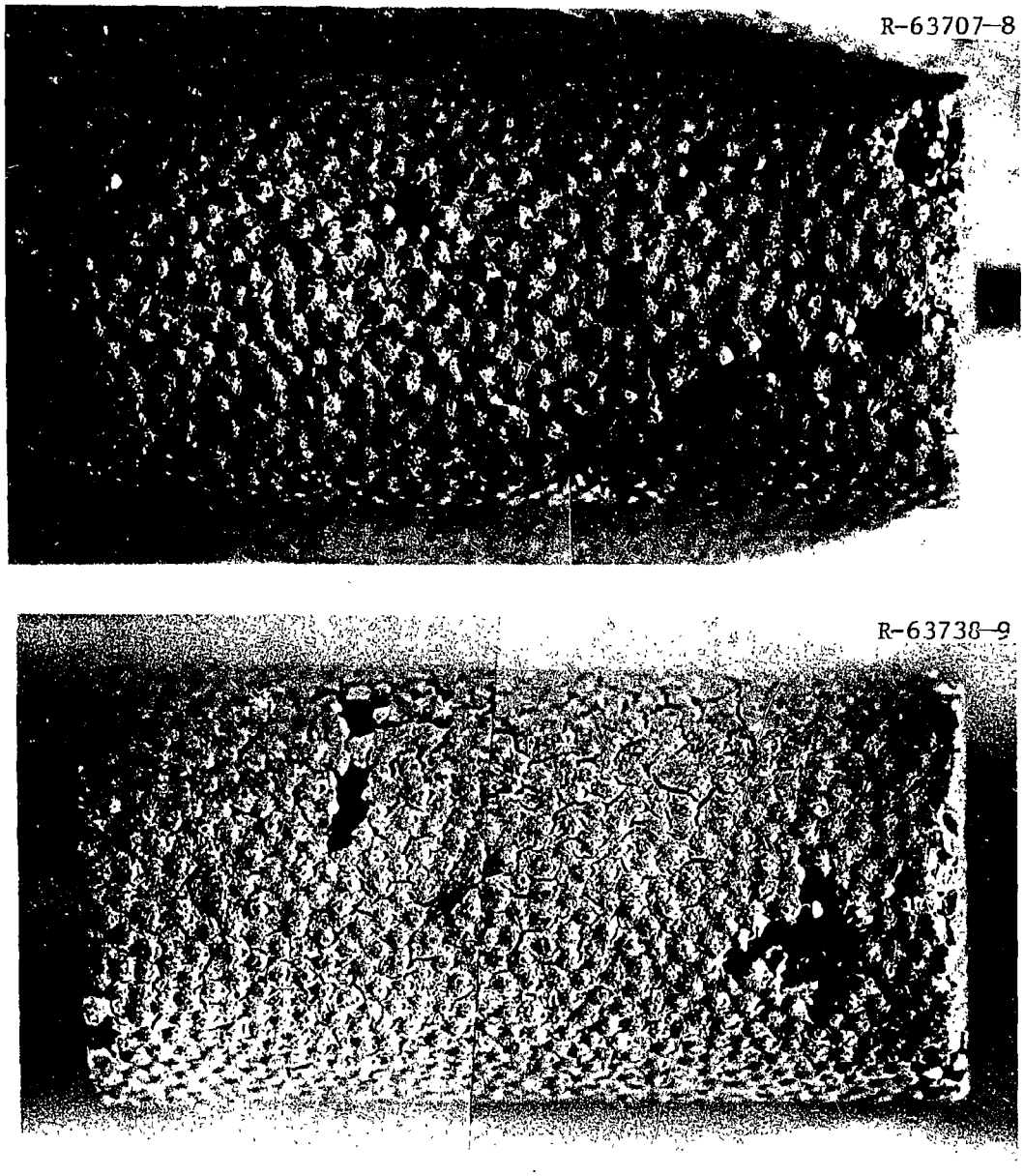

Fig. 16. Slug-Injected Rods 3A (Top) and 3C After Irradiation. 5×.

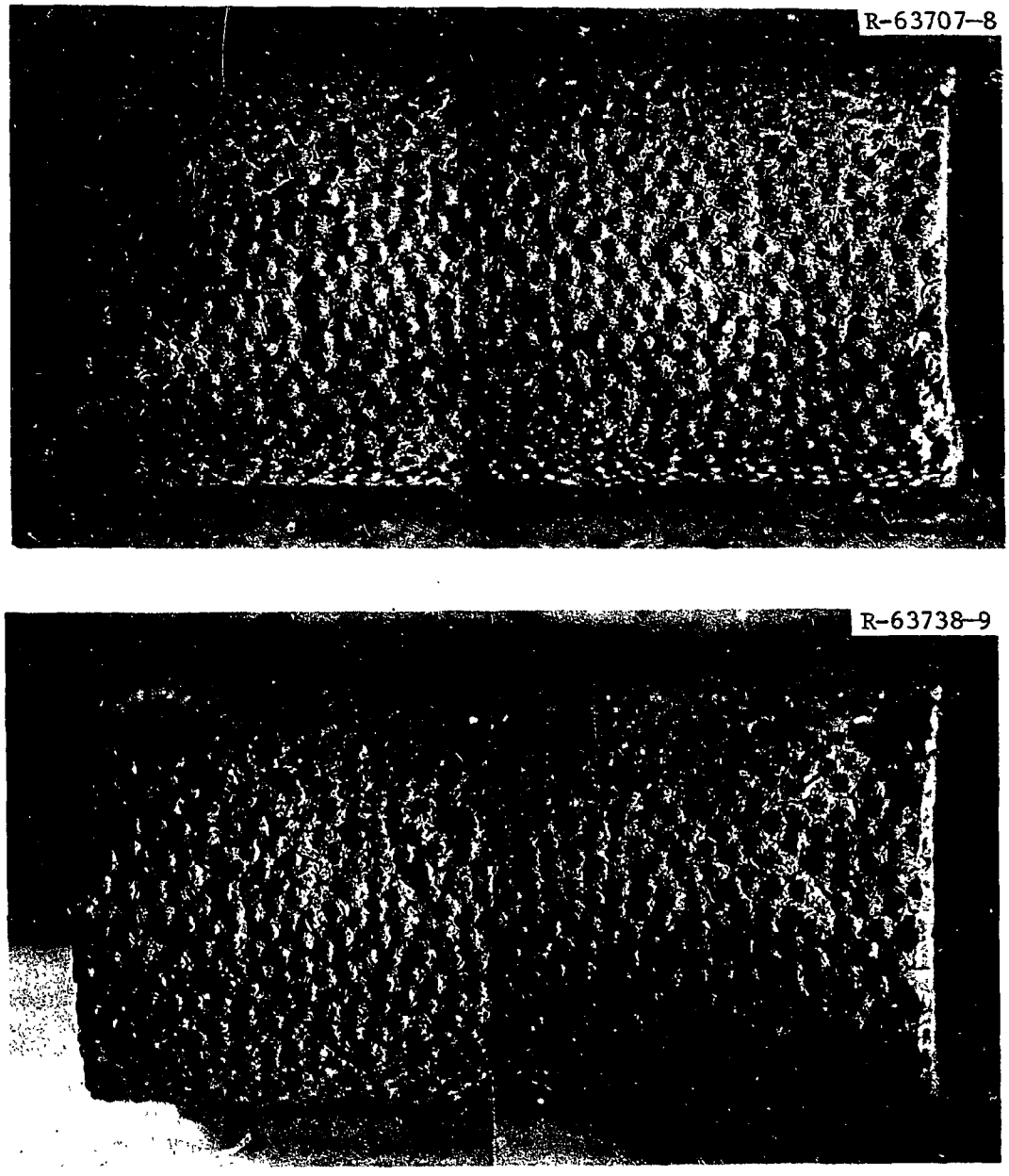

Fig. 17. Slug-Injected Rods 3B (Top) and 3D After Irradiation. 5×.

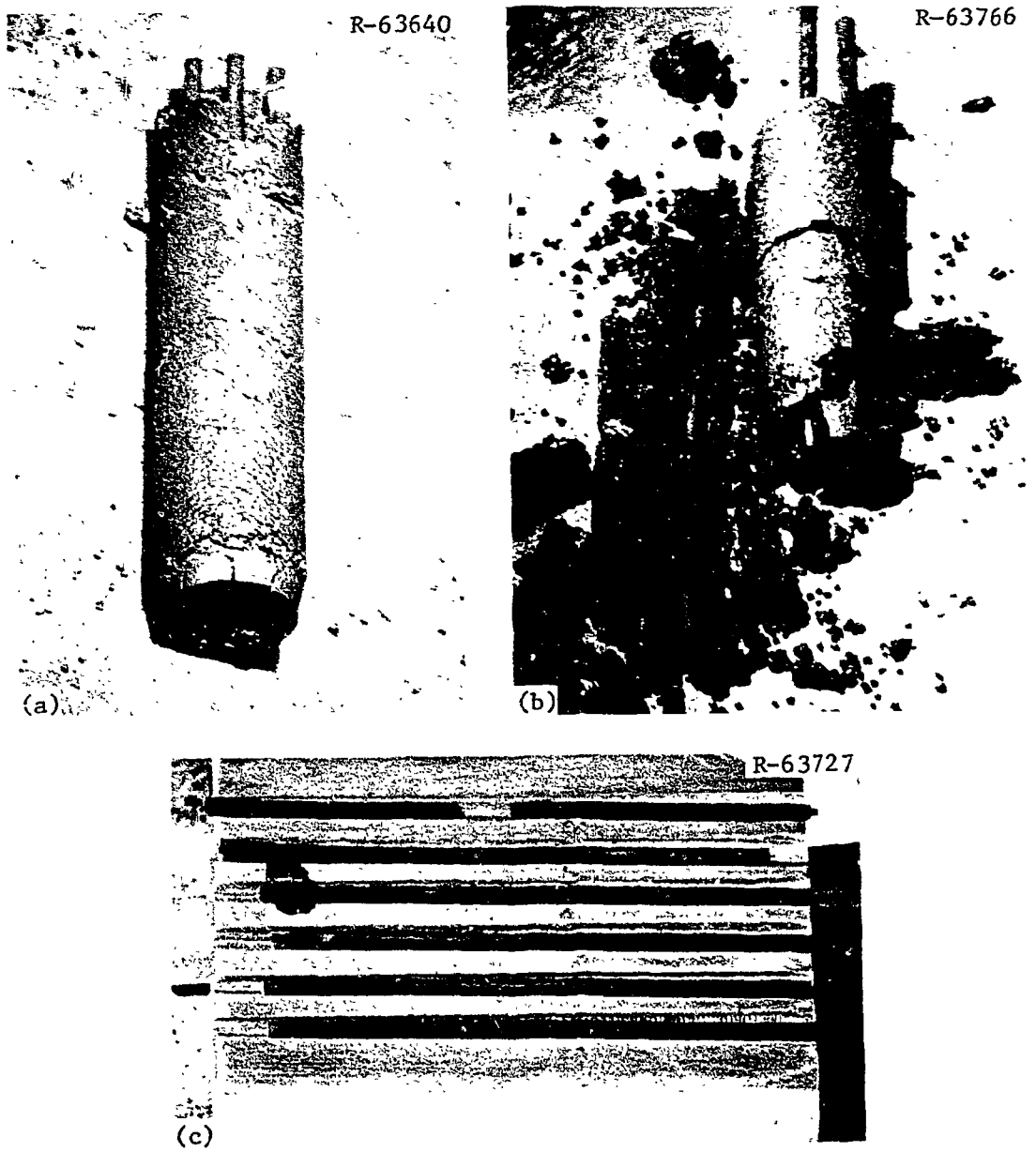

Fig. 18. Bonded Rod Holder 1C. 1.4×. (a) After removal from capsule. (b) After removing two graphite tubes. (c) Note tube 5 is broken and all tubes are distorted.

after removal from the capsule and after two of the graphite tubes that contained loose particles were removed from the rod. All six of the graphite tubes were recovered and identified (Fig. 18).

Attempts to recover the loose particles from the graphite tubes contained in the bonded-bed holder 1C were less than successful. Although a special vacuum pick-up fixture was fabricated for extracting the particles from the graphite tubes, a large number of the particles were lost because tube 6 fractured during irradiation and the grafoil end plugs fell out of some of the tubes during handling. The results of this recovery operation are given in Table 8; particles recovered are shown in Fig. 19. The particles from holders 1 and 2 were transferred to T. B. Lindemer of the Chemical Technology Division for fission-product release and gas-pressure measurements. The results will be reported separately.

Table 8. Loose Particles Contained in Graphite Tubes in Bonded Bed Holder 1C

Hole	Batch	Coating Type	Kernel Composition	Number in Tube	Number Recovered	Failed (%)
1	OR-1909	Biso	4:1(Th,^{235}U)O_2	75	37	0
2	OR-1910	Triso	4:1(Th,^{235}U)O_2	75	68	1.5
3	Pu-291	Biso	4:1(Th,^{233}U)O_2	75	a	100%
4	Pu-295 OR-1562	Triso Biso	$^{233}UO_2 - UC_2$ ThO_2	28 47	38[b]	c
5	Pu-296 OR-1562	Triso Biso	$^{233}UC_2$ ThO_2	25 48	28[b]	d
6	Pu-297 OR-1562	Triso Biso	$^{233}UC_2$ + C ThO_2	22 48	1[b]	

[a]Actual count of particles could not be determined, see Fig. 19.

[b]The two types of particles were indistinguishable by visual examination.

[c]Coating debris indicated a significant number of particles had failed.

[d]Single line fractures and "cascade-type" failures by kernels from adjacent failed particles indicated a significant number of particles had failed.

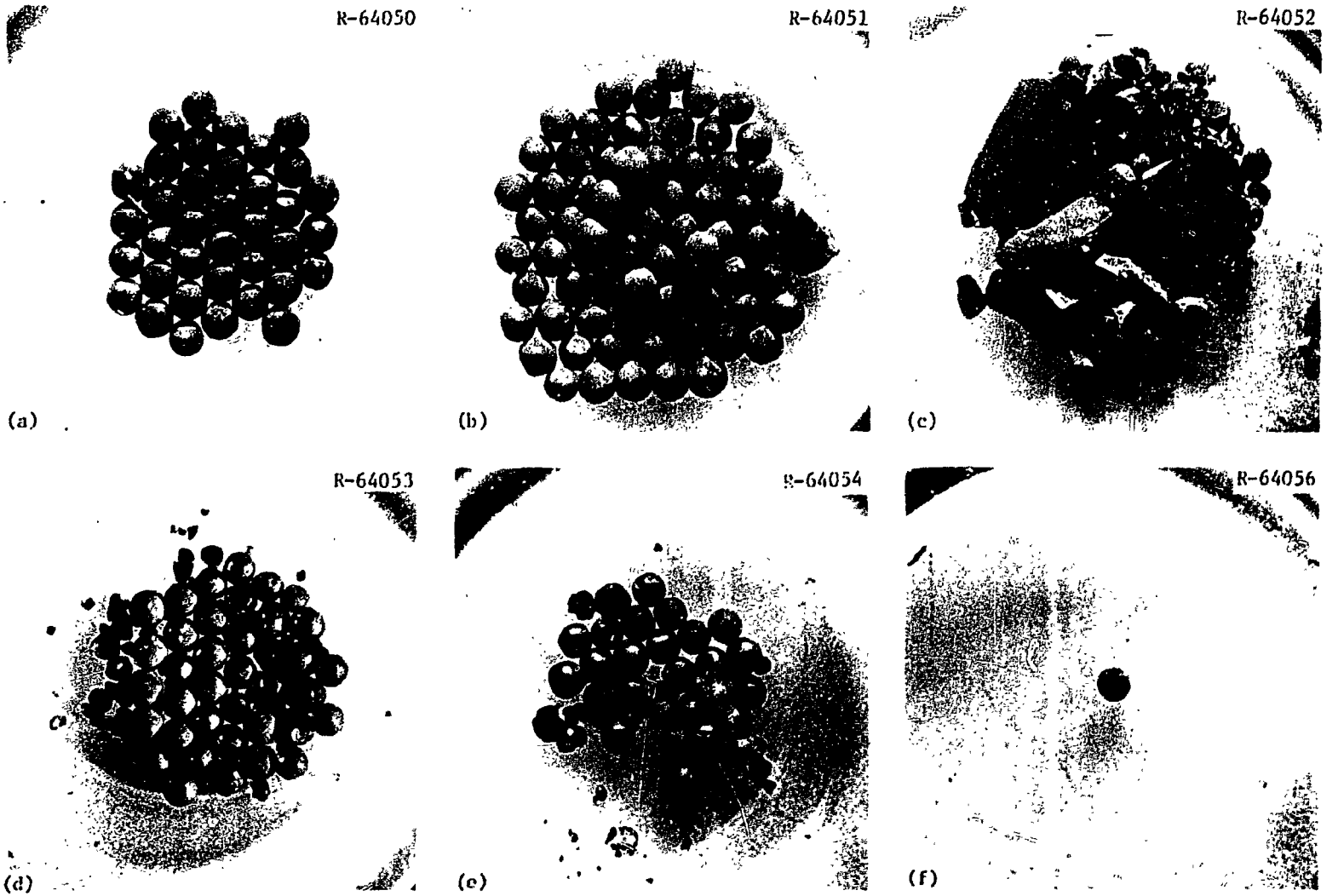

Fig. 19. Appearance of Loose Particles Recovered from Graphite Tubes Contained in Bonded Bed Holder 1C. 10×. (a) OR-1909. (b) OR-1910. (c) Pu-291. (d) Pu-295, OR-1562. (e) Pu-296, OR-1562. (f) Pu-297, OR-1562.

Dimensional Inspection

Each ORNL fuel rod was inspected by measuring the diameters at the top, midlength, and bottom at 0 and 90°; and a maximum length was determined. A tabulation of dimensional changes and fast fluences is given in Table 9. The detailed inspection sheets are reproduced in Appendix B. Significant shrinkage occurred for all of the rods and, for the majority, anisotropically.

The Poco graphite sleeve that contained the fuel rods was measured and the results were compared with the as-machined dimensions. The dimensional changes of both the graphite sleeve and the fuel rods were used in the detailed thermal analysis of this capsule, as described in Appendix A.

Table 9. Dimensional Changes and Fast Fluences for Fuel Rods from HRB-6

Fuel Rod	Fast Fluence, >0.18 MeV (n/cm^2)	Dimensional Change, %		$\frac{\Delta D}{D}/\frac{\Delta L}{L}$	Matrix Density[c] (g/cm^3)	Particle Volume (%)
		Diameter	Length			
1A[a]	5.86×10^{21}	−2.95	−3.76	0.78	1.50	43
1B[a]	6.89	−3.45	−3.57	0.97	1.62	44
3A[b]	7.22	−3.19	−4.74	0.67	0.81	61
3B[b]	6.72	−4.72	−5.54	0.35	0.76	61
3C[b]	6.09	−3.41	−4.59	0.74	0.81	62
3D[b]	5.43	−4.56	−4.74	0.96	0.74	62

[a]Extruded rods.

[b]Slug-injected rods.

[c]Unirradiated.

Metallographic Examination

One of the prime objectives of this experiment was to compare the relative performance of Biso-coated 4:1 (Th,^{233}U)O_2 with Biso-coated 4:1 (Th,^{235}U)O_2 in slug-injected rods. This capsule also permitted a comparison of Triso-coated 4:1 (Th,^{235}U)O_2 with Biso-coated 4:1 (Th,^{235}U)O_2 in extruded rods. Although the extruded rods and the slug-injected rods were irradiated at nearly equivalent flux conditions, the extruded rods operated at a lower temperature because of their higher matrix thermal conductivity (due to higher matrix density).

Transverse sections were taken through the extruded rods approximately 1/2 in. from the bottom of rod 1A and about 1/2 in. from the top of 1B to allow a comparison of the performance of the particles contained in the two rods. Metallographic examination of the section through rod 1A, which contained the Triso-coated 4:1 (Th,^{235}U)O_2 fissile particles, revealed no failures of either the fissile or fertile particles. The fissile kernels contained numerous relatively small fission-gas bubbles, and intermittent plastic flow of the kernel through the fission recoil zone of the buffer coating was noted. No evidence of amoeba was noted in either the fissile or fertile kernels. Typical fissile particles from the maximum and minimum temperature regions of fuel rod 1A are shown in Figs. 20 and 21.

The results from the metallographic section through rod 1B, which contained Biso-coated 4:1 (Th,^{235}U)O_2 fissile particles, were similar to those observed in rod 1A. One difference noted was that there was slight evidence[9] of amoeba in a few of the fissile kernels. A typical fissile particle is shown in Fig. 22.

Transverse sections were made near the midlength of two of the slug-injected rods (specifically, 3A and 3B) and examined metallographically. The section through rod 3A revealed that the majority of the coatings on the ^{233}U-bearing kernels had failed. A typical fissile particle is shown in Fig. 23. Examination of the coatings revealed that a very dense buffer had been applied on the kernels and that a variation in properties could be seen in the outer coatings when viewed under polarized light. Thus, the coatings failed during irradiation as a result of poor coating characteristics. The kernels contained numerous relatively small fission-gas bubbles and metallic fission-product globules. Migration of the kernels up the thermal gradient for a maximum distance of 20 μm was apparent. No coating failures were noted for the ^{235}U-bearing kernels in slug-injected rod 3B. The appearance and performance of the fissile particles in rod 3B was similar to that described for 3A. A typical fissile particle located near the inner surface of rod 3B is shown in Fig. 24. A high magnification view of the cold side of this particle showing the rejected carbon and the fission-recoil zone is shown in Fig. 25.

The Biso-coated ThO_2 fertile particles used in HRB-6 fuel rods showed no evidence of kernel migration or other deleterious effects from the irradiation test.

DISCUSSION AND CONCLUSIONS

The fissile kernels in the HRB-6 bonded fuel rods were $(Th_{0.8}U_{0.2})O_2$. The uranium was either ^{233}U or fully enriched ^{235}U. At the time the experiment was planned, the reference HTGR recycle kernel was dense mixed oxide with a Th/U ratio of 4:1. The experiment was planned as a test of reference recycle fuel. However, after the experiment was completed, a change was made in the reference, and the dense mixed oxide

---

[9]The threshold of observation for amoeba is movement of ∿2—3 μm.

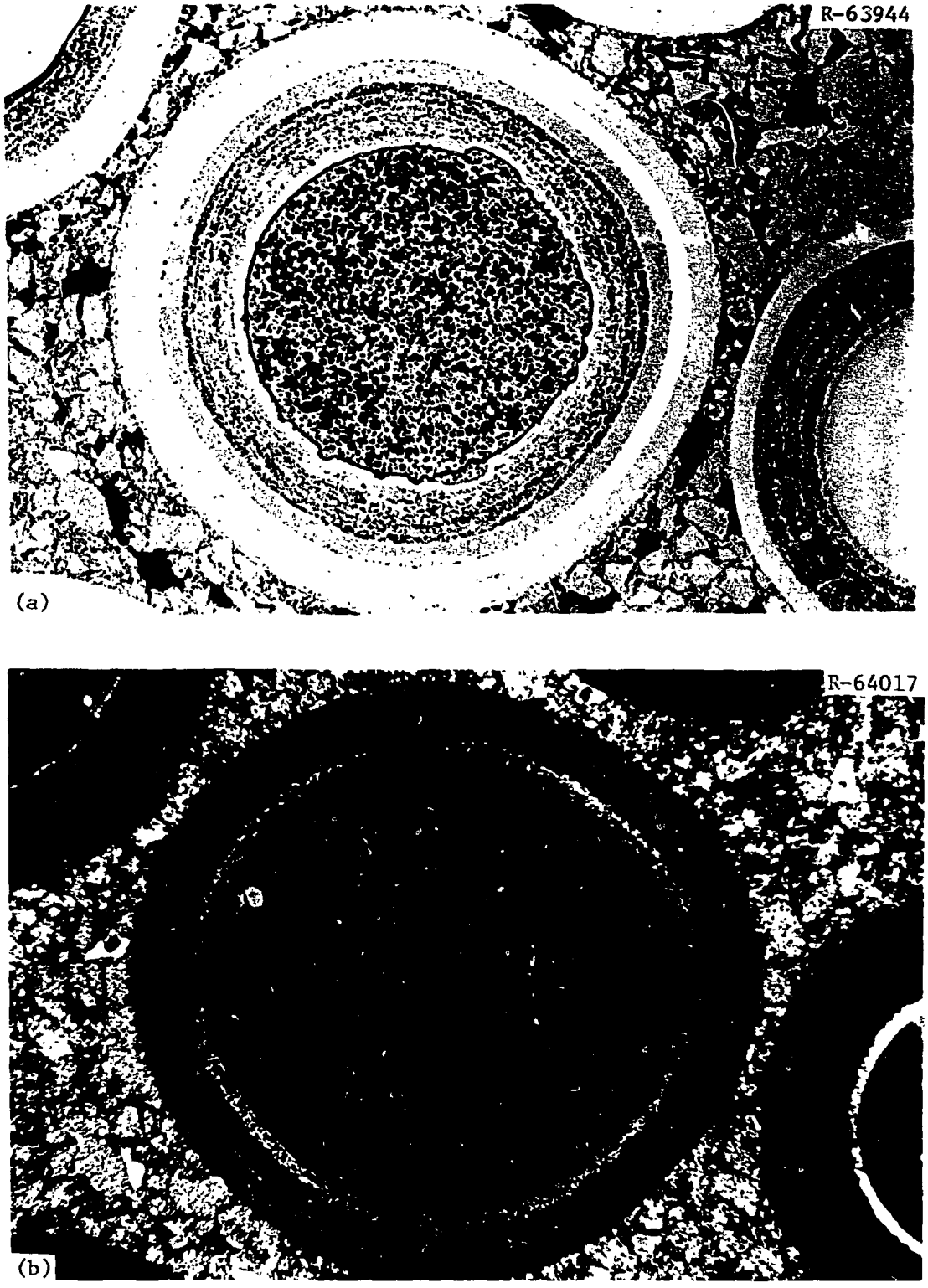

Fig. 20. Irradiated Triso-Coated Fissile Particle in Extruded Fuel Rod 1A. The center of this particle is 1000 μm from the outer surface of the fuel rod. 150×. (a) Bright field. (b) Polarized light.

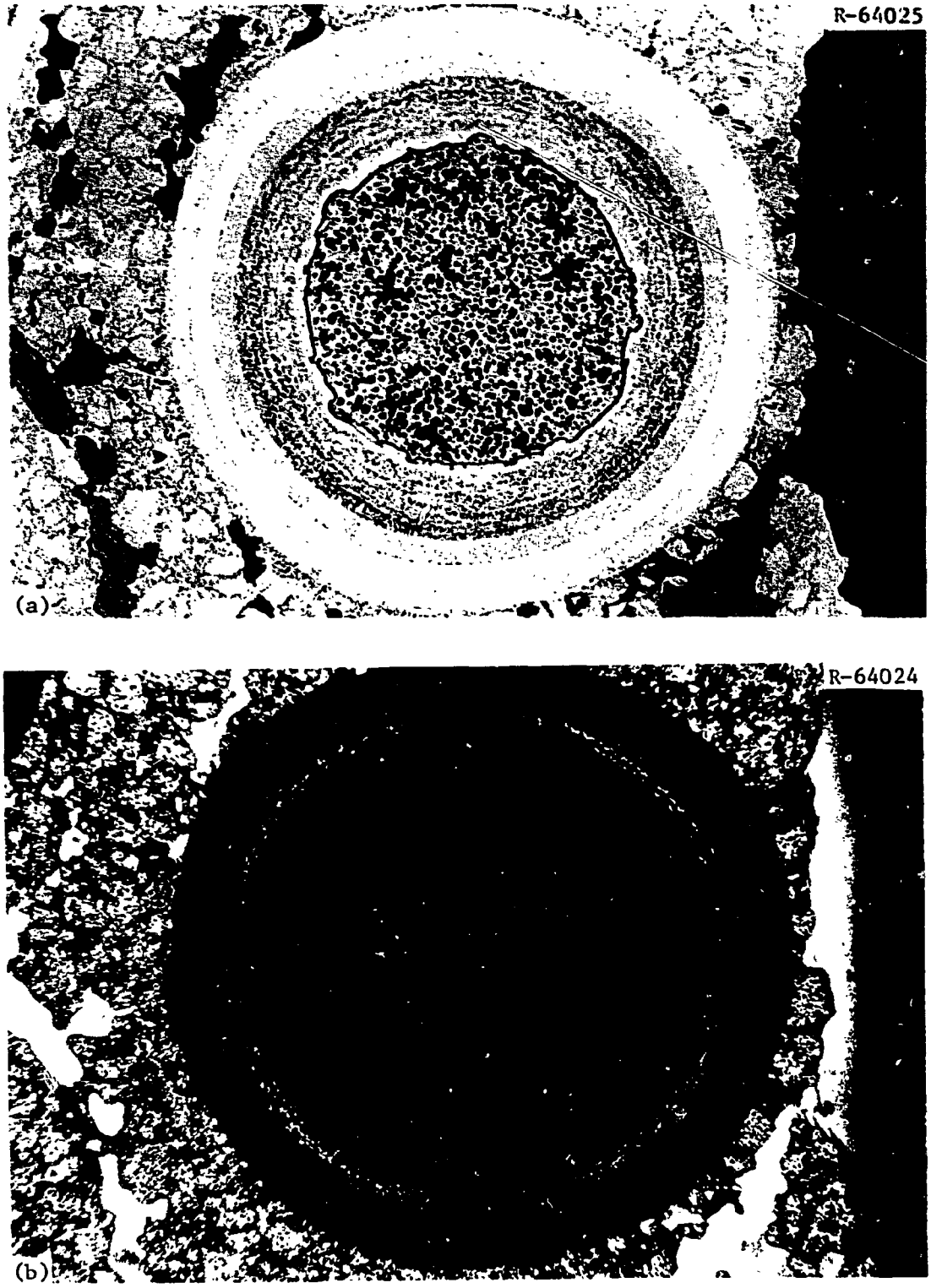

Fig. 21. Irradiated Triso Fissile Particle in Extruded Fuel Rod 1A. This particle is located at the maximum temperature region of the fuel rod; the inner surface of the rod can be seen in this figure. 150×. (a) Bright field. (b) Polarized light.

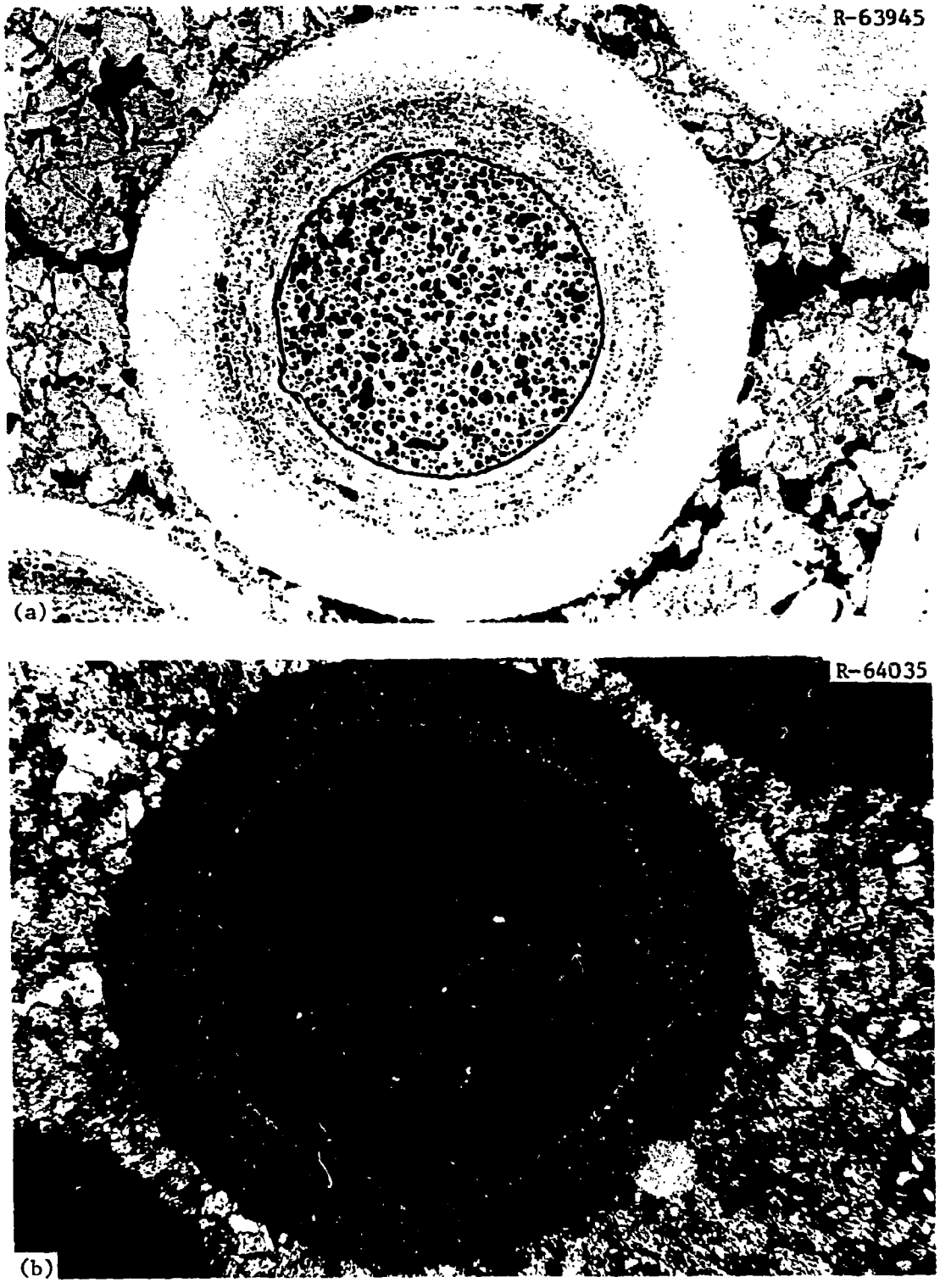

Fig. 22. A Typical Biso-Fissile Particle in Extruded Fuel Rod 1B. 150×. (a) Bright field. (b) Polarized light.

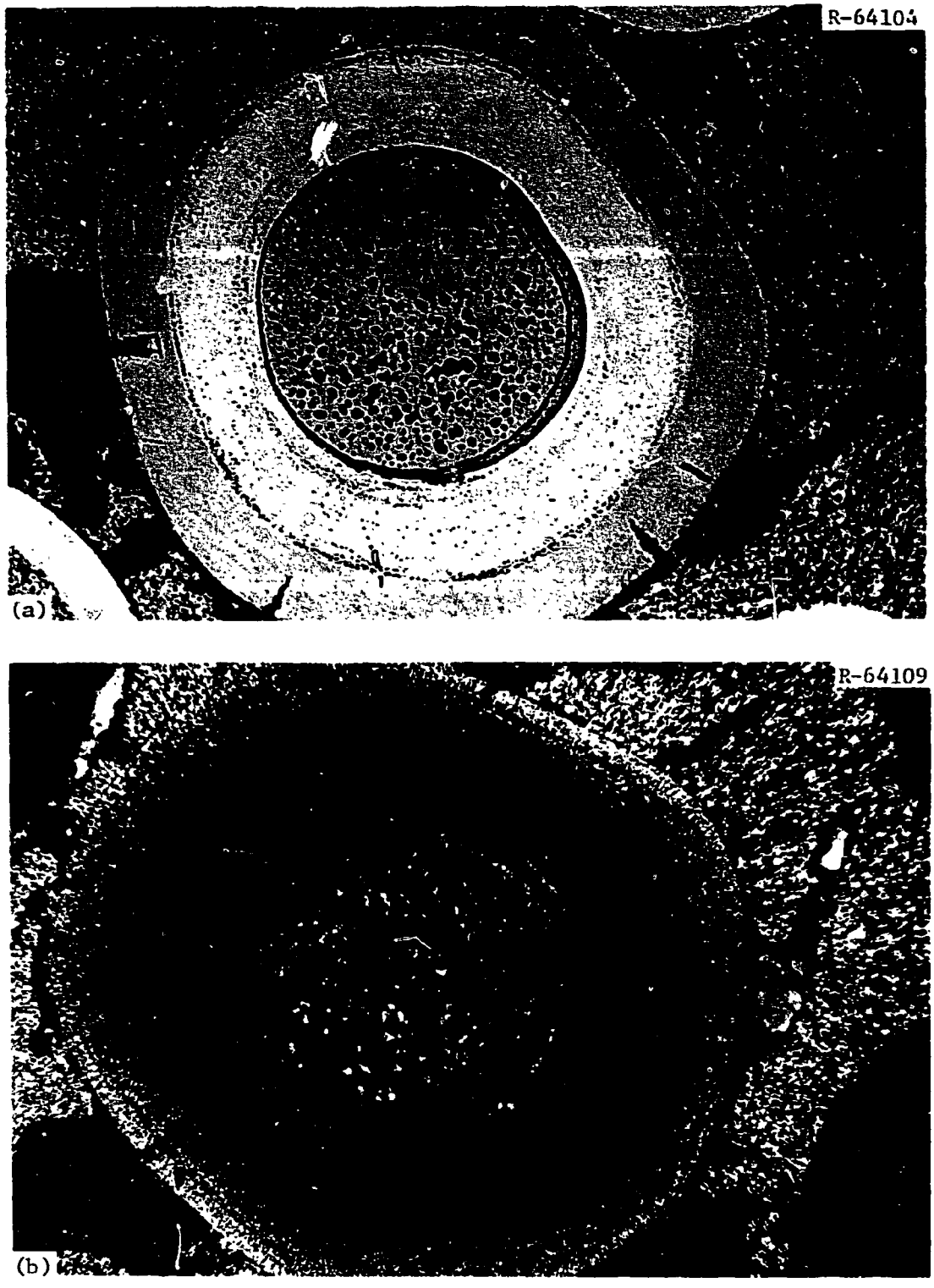

Fig. 23. Typical Biso-Coated 4:1 (Th,^{233}U)O_2 Fissile Kernel in Slug-Injected Fuel Rod 3A That Shows Evidence of "Amoeba." The failed coatings were a result of poor coating properties. 150×. (a) Note the dense buffer layer and (b) the anisotropy of the outer coating (polarized light).

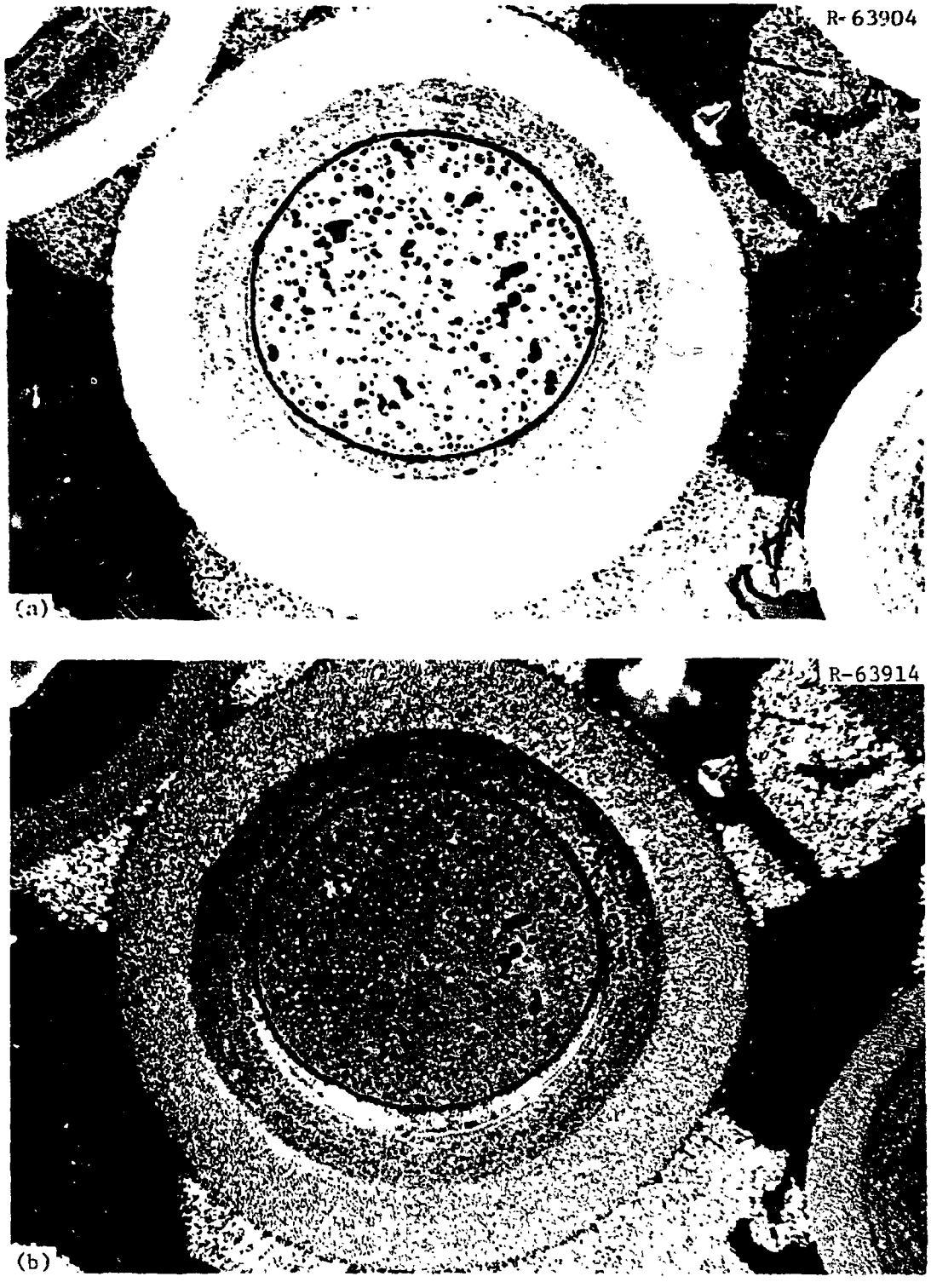

Fig. 24. Typical Biso-Coated 4:1 (Th, $^{235}U)O_2$ Kernel in Slug-Injected Fuel Rod 3B. 150×. (a) Bright field. (b) Polarized light.

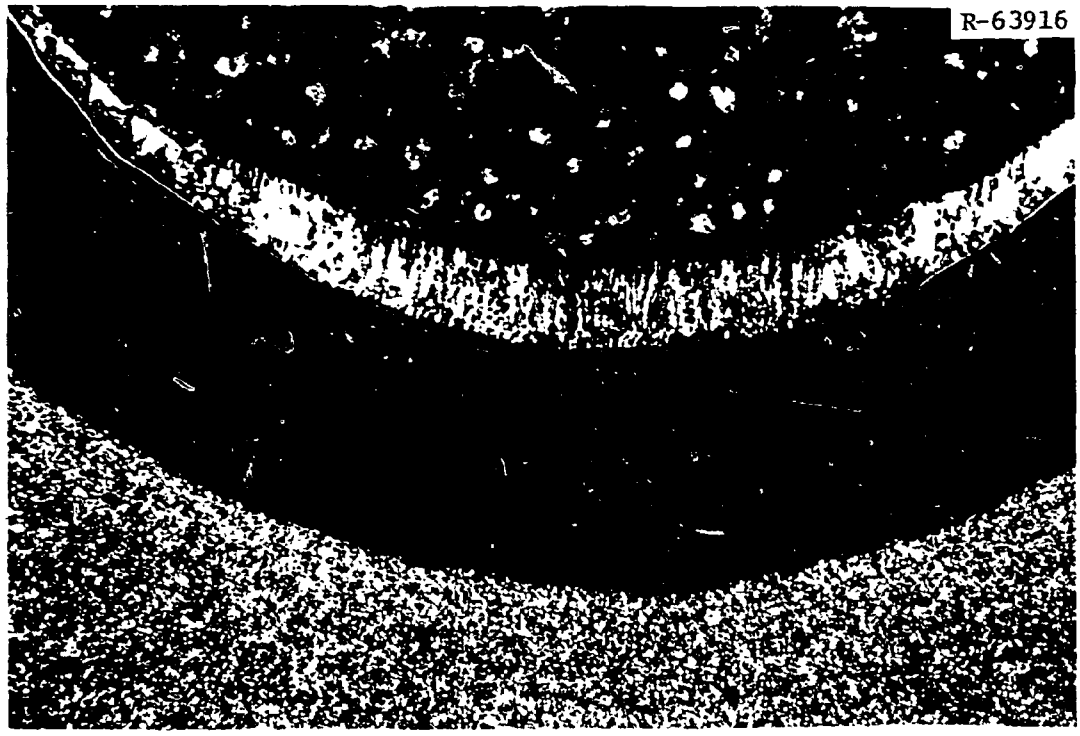

Fig. 25. Rejected Graphite Between the Kernel and Buffer on the Cold Side of the Particle Shown in Fig. 24. Polarized light. 500×.

kernel was replaced with a porous kernel derived from ion-exchange resin. Some important information was derived from the experiment to support the recycle development program, in spite of this change in reference fuel. During the planning of the experiment it was assumed that the behavior of ^{233}U and ^{235}U under irradiation would be very nearly identical, because of the similarity in the fission-product spectra for the two isotopes. The results of the experiment proved this assumption to be valid for the mixed oxide fissile fuel. The coatings of the ^{233}U containing particles performed very badly. Numerous failures were noted during irradiation of the ^{233}U containing rods as shown in Fig. 23. However, this poor performance was attributed to bad coatings, not the performance of the kernels. There was no measurable difference in the thermal stability of the ^{233}U and ^{235}U kernels. This is shown in Fig. 26, which is a plot of the kernel migration coefficient vs reciprocal temperature for both types of kernel. A discussion on the meaning and

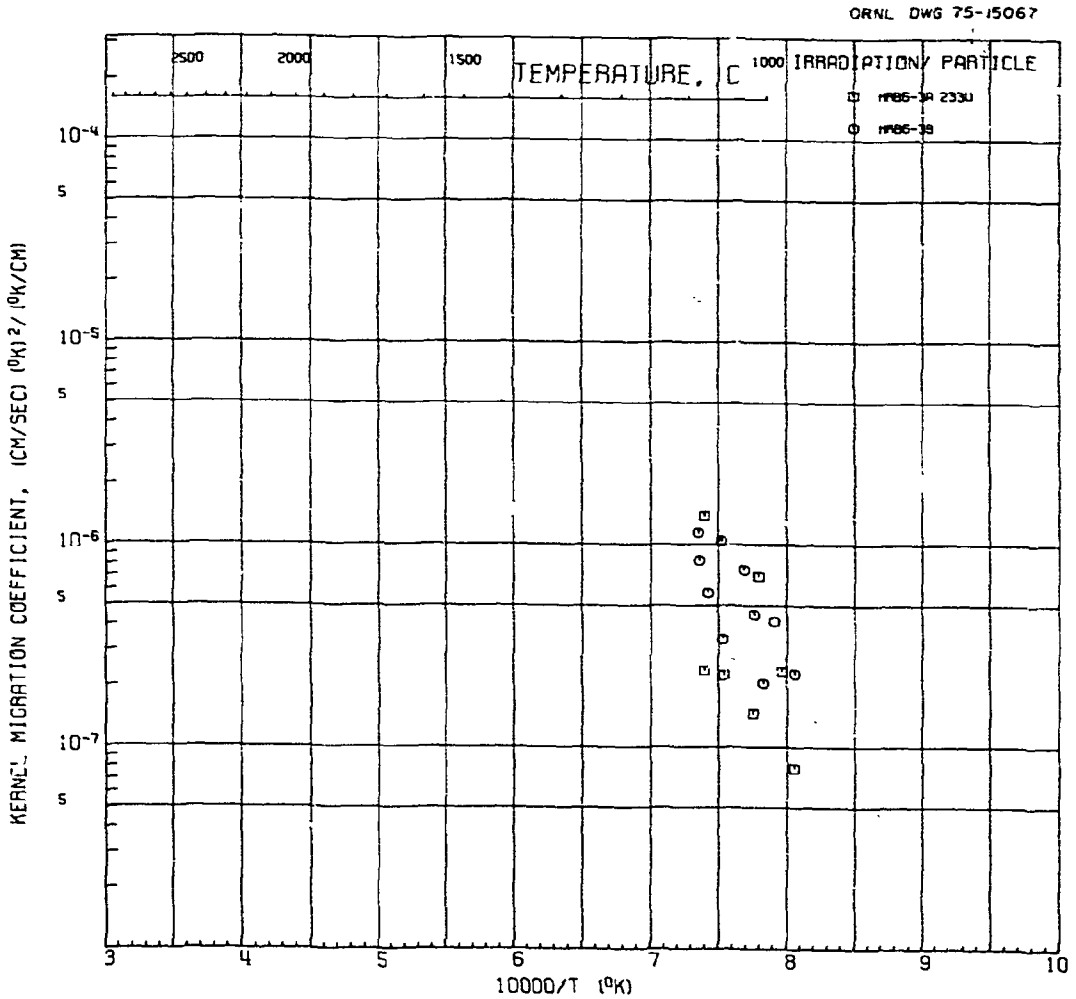

Fig. 26. Experiment HRB-6 Kernel Migration Coefficients for $(Th_{0.81}U_{0.19})O_2$ Containing Either ^{233}U or ^{235}U.

measurement of the kernel migration coefficient has been reported by Lindemer.[10,11] The data for specimen 3A (containing ^{233}U) seems to be more scattered than that for specimen 3B. This is not considered significant, however, in view of the large amount of scatter encountered in all

[10]T. B. Lindemer and H. J. de Nordwall, *An Analysis of Chemical Failure of Coated UO_2 and Other Oxide Fuels in the High-Temperature Gas-Cooled Reactor*, ORNL-4926 (January 1974).

[11]T. B. Lindemer and R. A. Olstad, *HTGR Fuel Kernel Migration Data for the Th-U-C-O System as of April 1, 1974*, ORNL-TM-4493 (June 1974).

kernel migration plots.[10,11] The thermal stability of the mixed oxide fuel contained in the HRB-6 experiment is compared with data from other experiments in Fig. 27. The information contained in Fig. 27 is considered to be preliminary.[12] There is so much scatter in the data, that to say whether the HRB-6 data are consistent with the data from previous experiments is difficult. Much of the scatter is due to uncertainties with the temperatures and temperature gradients of the fuel rod specimens during irradiation. Both these factors are used in computing the kernel migration coefficient. Work in this area is continuing, and a more detailed analysis of the thermal migration data will be published by Lindemer and Pearson.

---

[12]T. B. Lindemer and R. L. Pearson, unpublished work, July 1975.

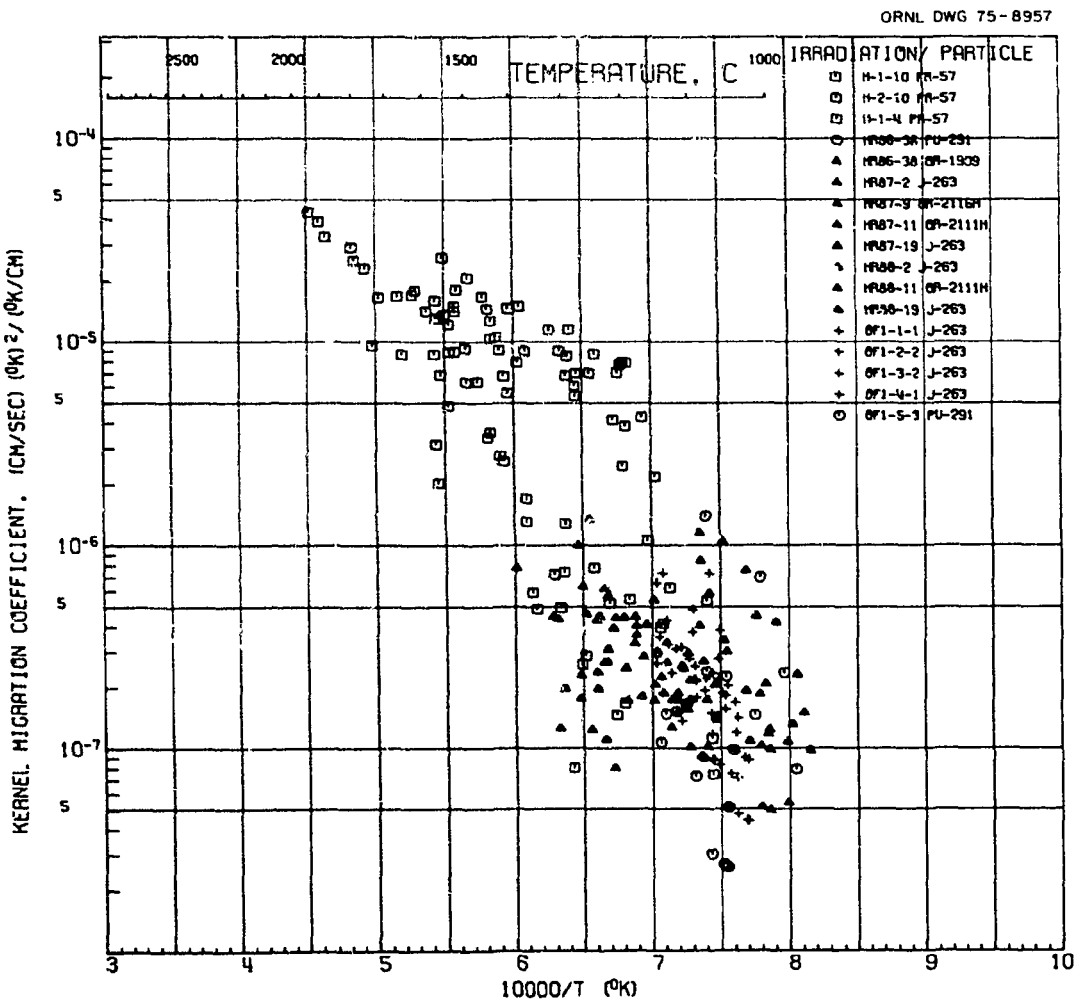

Fig. 27. Summary of Kernel Migration Data for Mixed Oxide Kernels with Th/U ∿4:1.

The migration rates measured to date for the mixed oxide kernels indicate marginal performance of this fuel for commercial HTGR application. However, demonstration of the equivalence of ^{233}U and ^{235}U is very important to the recycle development program because it permits substitution of ^{235}U in tests conducted in support of process and equipment development. Testing with ^{233}U is enormously more expensive than with ^{235}U because of the kernel and fuel rod fabrication difficulties associated with gamma emitting ^{233}U. While this experiment was not designed to establish full equivalence, it is an important preliminary result. The change in reference from the dense mixed oxide to the WAR derived kernel will necessitate further testing; and full equivalency will require testing over a variety of fuel compositions.

The experimental objectives associated with the six columns of loose particles contained in specimen 1C were not met. The bonded-bed holder, the graphite tubes, and the loose particles were in very poor condition after the irradiation. This poor performance, coupled with the difficulties encountered in retrieving and examining loose particles in this holder configuration caused abandonment of further attempts at combining loose particles and fuel rods in HRB capsules. Studies of fission product retention in the loose particles that did survive irradiation (objective 2) will be reported separately.

The very good performance of the fuel rods fabricated by extrusion as compared to the slug-injected rods was demonstrated again in this experiment. A very limited amount of irradiation experience has been accumulated at ORNL on extruded fuel, but in all cases (8 fuel rods in 3 different HRB capsules) the condition of the extruded fuel after irradiation to fast fluence levels expected in an HTGR has been excellent. Very little debonding of the rods, and less thermal migration of the dense oxide kernels (amoeba) was seen. This last observation is due to the lower temperature and temperature gradients in the extruded rods, operating at nominally the same power output as the slug-injected rods. The superior performance of the extruded rods is due to the higher thermal conductivity of the dense continuous matrix.

The dimensional stability of the HRB-6 fuel rods was anticipated for the Biso-Biso system. The two slug injected fuel rods fabricated with ^{233}U in a glove box had somewhat higher matrix density, and therefore experienced less densification under irradiation than the companion specimens, fabricated with ^{235}U in a contact facility. This resulted in somewhat higher operating temperatures in the ^{233}U bearing fuel rods.

The ultrasonic center-line thermometer (objective 5) did not perform well in this experiment. On the basis of this experience, and previous failures with this device, it has been abandoned.

ACKNOWLEDGMENTS

The authors wish to acknowledge the efforts of many people who made significant contributions to the planning, execution, and evaluation of this irradiation test. W. P. Eatherly and J. L. Scott of the Metals and Ceramics Division, and J. A. Conlin of the Reactor Division participated in the planning and design of the experiment. Conlin also assisted

in the construction of the capsule; W. P. Eatherly and J. L. Scott also participated in the evaluation of results. R. A. Bradley and W. H. Miller, Jr. of the Metals and Ceramics Division fabricated and characterized the slug-injected fuel rods. J M Robbins and D. E. Rosson of the Metals and Ceramics Division fabricated and characterized the extruded rods and the intrusion bonded rod. The fissile and fertile particles were coated and characterized by R. L. Beatty of the Metals and Ceramics Division. The dosimetry and thermometry of this capsule were provided by H. T. Kerr of the Reactor Division and R. L. Shepard of the Instruments and Controls Division, respectively. The metallography of the unirradiated loose particles and fuel rods was performed by M. D. Allen and C. E. Zachary of the General Metallography Group, and the remote metallography was performed by N. M. Atchley and L. G. Shrader of the Radiation and Electron Metallography Group of the Metals and Ceramics Division. The authors also acknowledge the assistance of those who helped with the preparation of this report: R. H. Lafferty for technical editing and Judy Young for typing and makeup.

APPENDIX A

THERMAL ANALYSIS

The body of this report contains plots of the calculated temperatures for selected specimens as a function of time through eight irradiation cycles in the HFIR. The calculations of these temperatures are rather involved, and the details have been described in a topical report.[1] Some of the details of the calculation for the HRB-6 capsule are contained in this appendix.

As described earlier, the HRB capsules contain a number of Chromel-Alumel thermocouples in the graphite sleeve adjacent to the fuel specimens. These thermocouples are used to control the operating temperature of the fuel. The control is achieved by adjusting the composition of the helium-neon sweep gas which flows through the capsule. The gas sweeps the gap between the fuel and the graphite sleeve and the gap between the sleeve and the stainless steel capsule wall. The composition of the gap is adjusted to give the desired temperature reading in the Chromel-Alumel thermocouple selected for control. The composition of the sweep gas can be measured by the relative volumes of helium and neon flowing from storage tanks, but this measurement is rather crude. Better values are obtained by calculation from the thermocouple data. Another aspect of the thermal analysis is calculation of the fission heat rate as a function of time from the fuel specimens. The neutron flux characteristics of the irradiation facility cause this parameter to vary with time. Methods are available to directly calculate the heat rates,[2] but uncertainty about the cross sections, and the exact shape of the neutron flux vs time curve at all axial locations make these methods somewhat unreliable. Much of this information is described elsewhere.[3] A more reliable method of calculating the fission heat rates is to use the temperature data from the Chromel-Alumel thermocouples in conjunction with a mathematical model.[4] Once the sweep gas compositions and time dependent heat rates are known, the same model is used to calculate fuel temperatures. The time dependent changes in fuel and graphite sleeve geometries are taken into account in these calculations. The time dependent changes in the gamma heating rates for the graphite sleeve, the stainless steel capsule, and the fuel rods are also taken into account. A brief summary of this information is presented below.

---

[1] F. J. Homan, *Thermal Analysis of HTGR Fuel Rods Irradiated in the HFIR Removable Beryllium Facility*, report in preparation.

[2] H. C. Roland, *FABGEN — A Transient Power-Generation and Isotope Birth Rate Calculator*, ORNL-TM-4750 (April 1975).

[3] F. J. Homan et al., *Irradiation Performance of HTGR Fuel Rods in HFIR Experiment HRB-3 and ETR Experiment P13N*, ORNL-TM-4526 (October 1974).

[4] F. J. Homan, *HTRANS — A FORTRAN IV Computer Program for Thermal Analysis of Coated Particle Fuels*, report in preparation.

Figures A1 through A8 are the plots of fission heat rate in the fuel specimens vs time at the six axial locations where thermocouples are located in the graphite sleeve. A plot of the sweep gas composition vs time is shown in Fig. A9. The sweep gas is a mixture of neon and helium, and Fig. A9 shows the percentage helium in the mixture. The solid curves in Fig. A9 represent the gas composition measurements made from the flowmeter data. The points (open circles) represent the calculated gas composition using the HTRANS code[4] and the Chromel-Alumel thermocouple data.

Figure A10 shows the assumed dimensional changes for the fuel rods with time. The dimensional change measurements made during postirradiation examination were presented in the body of this report. The curves that were drawn through these points were constructed using the

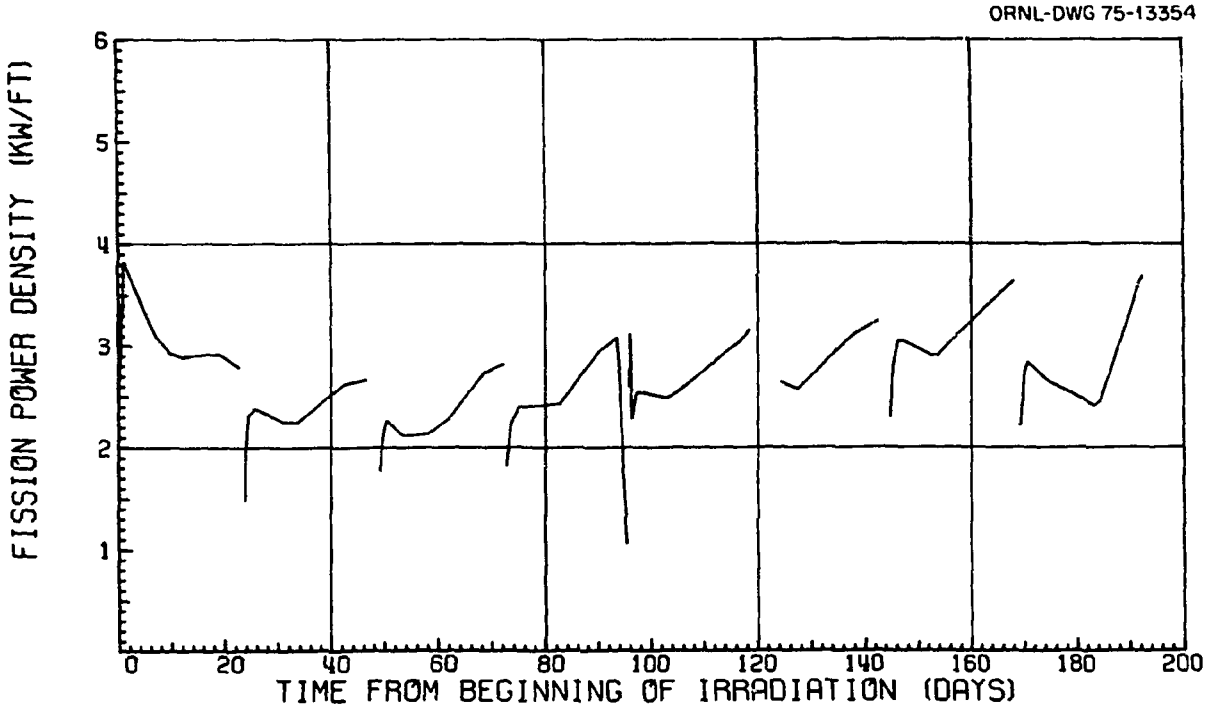

Fig. A1. Fission Heat Rate vs Time for HRB-6 at Axial Midpoint of Specimen 1B.

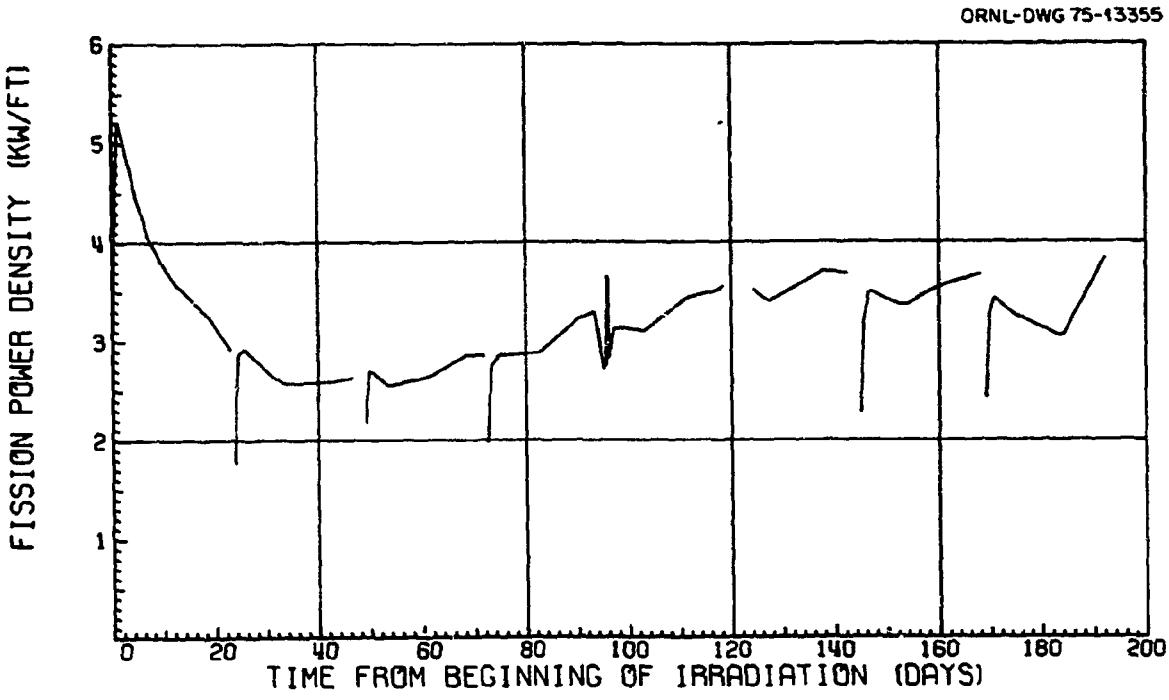

Fig. A2. Fission Heat Rate vs Time for HRB-6 at Axial Midpoint of Specimen 1C.

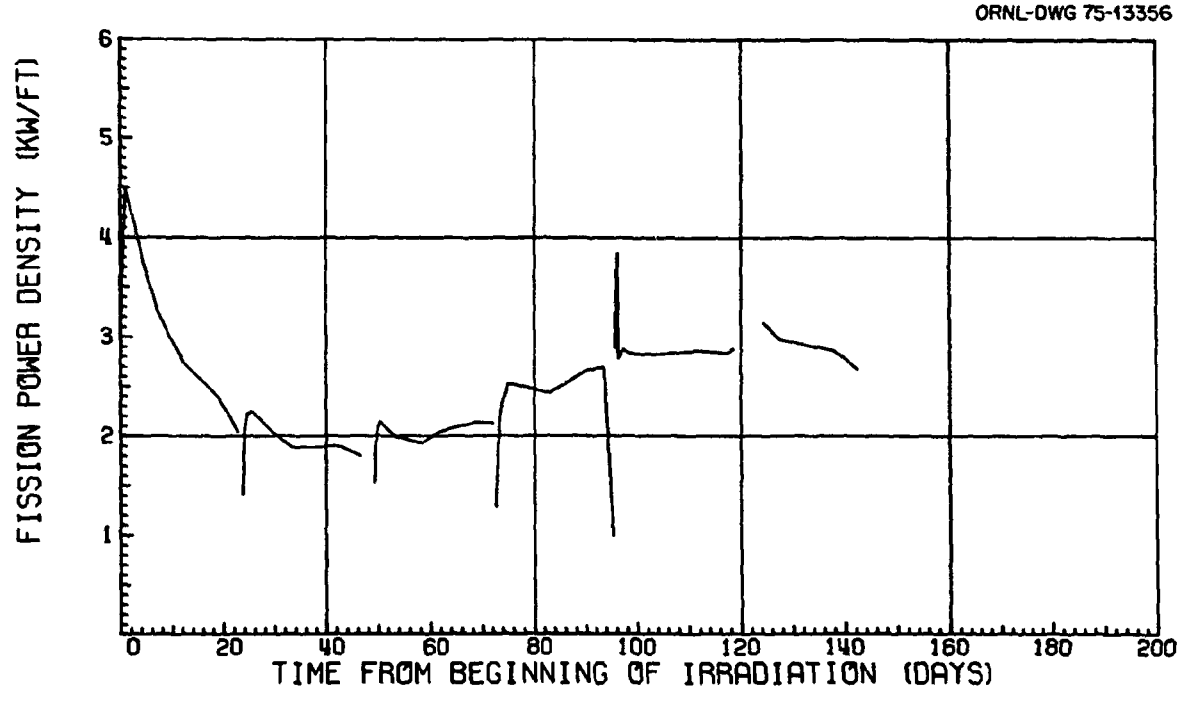

Fig. A3. Fission Heat Rate vs Time for HRB-6 at Axial Midpoint of Specimen 2B.

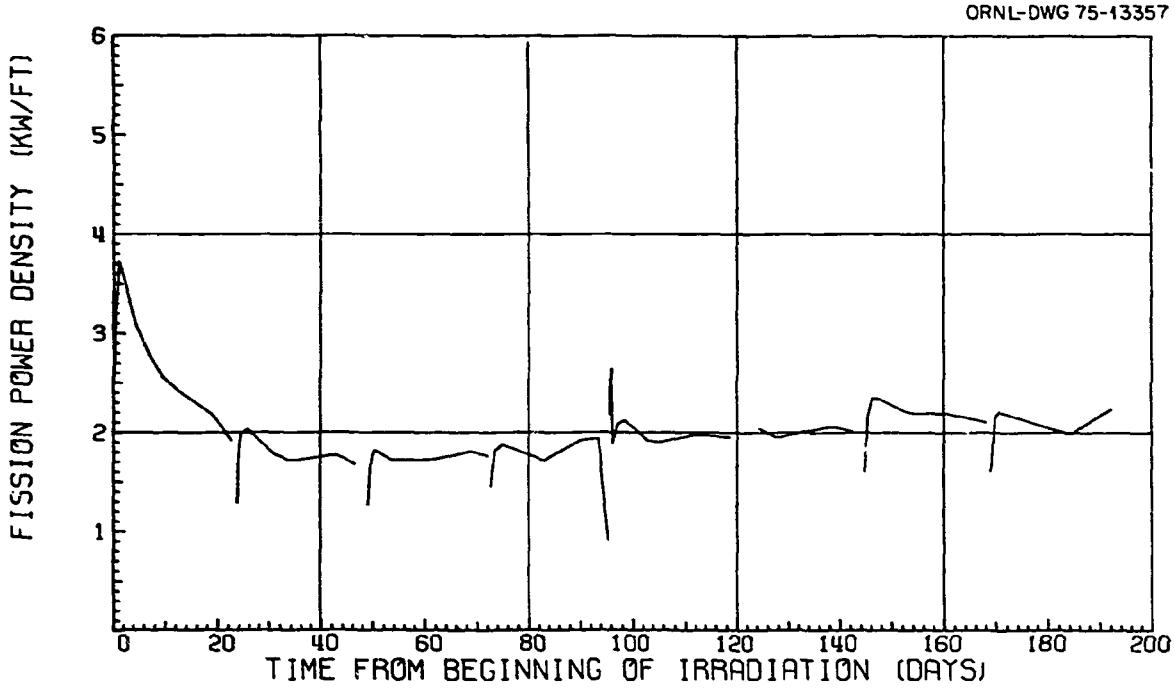

Fig. A4. Fission Heat Rate vs Time for HRB-6 at Axial Midpoint of Specimen 3A.

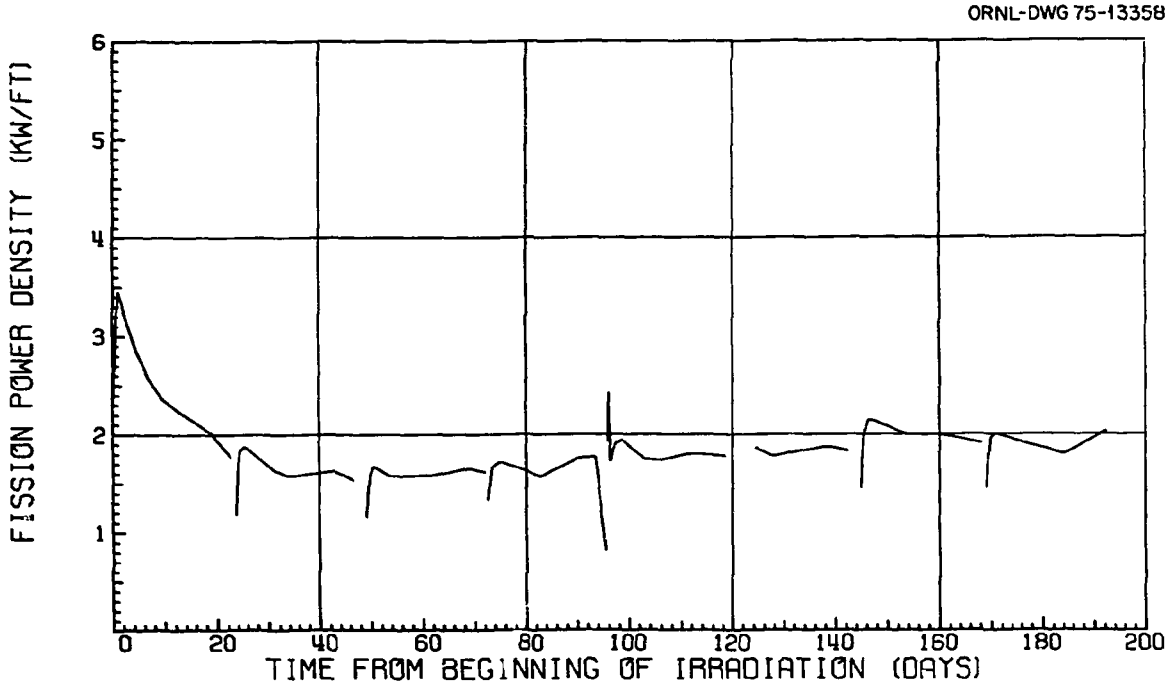

Fig. A5. Fission Heat Rate vs Time for HRB-6 at Axial Midpoint of Specimen 3B.

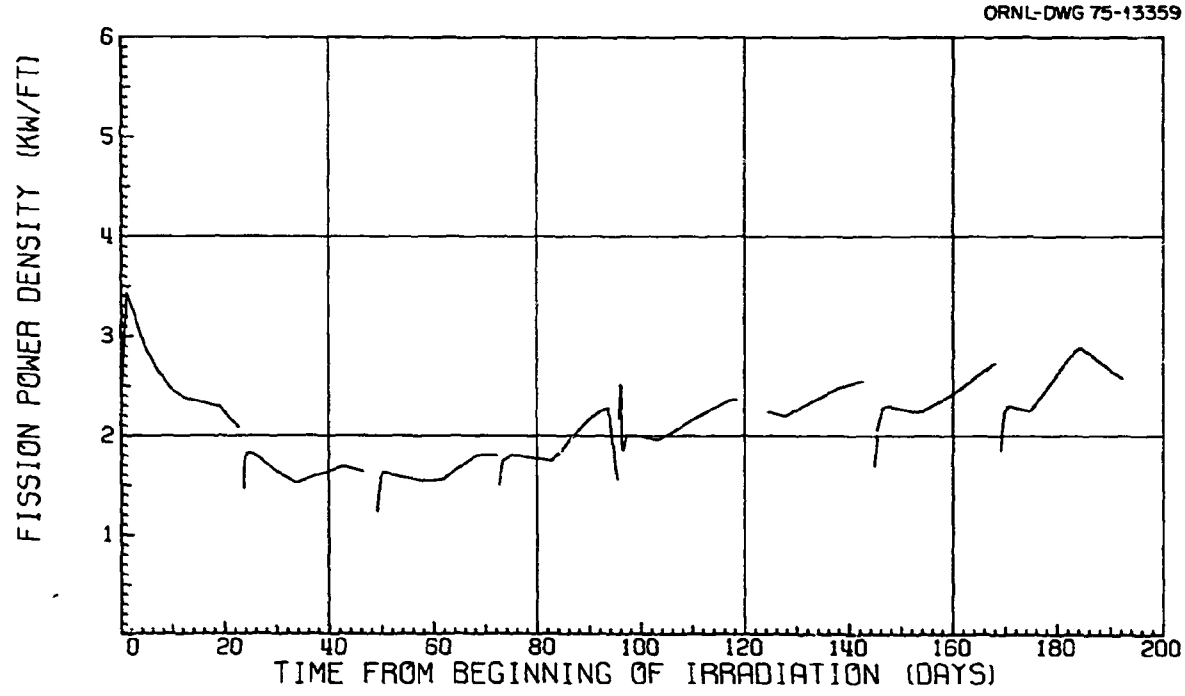

Fig. A6. Fission Heat Rate vs Time for HRB-6 at Axial Midpoint of Specimen 3C.

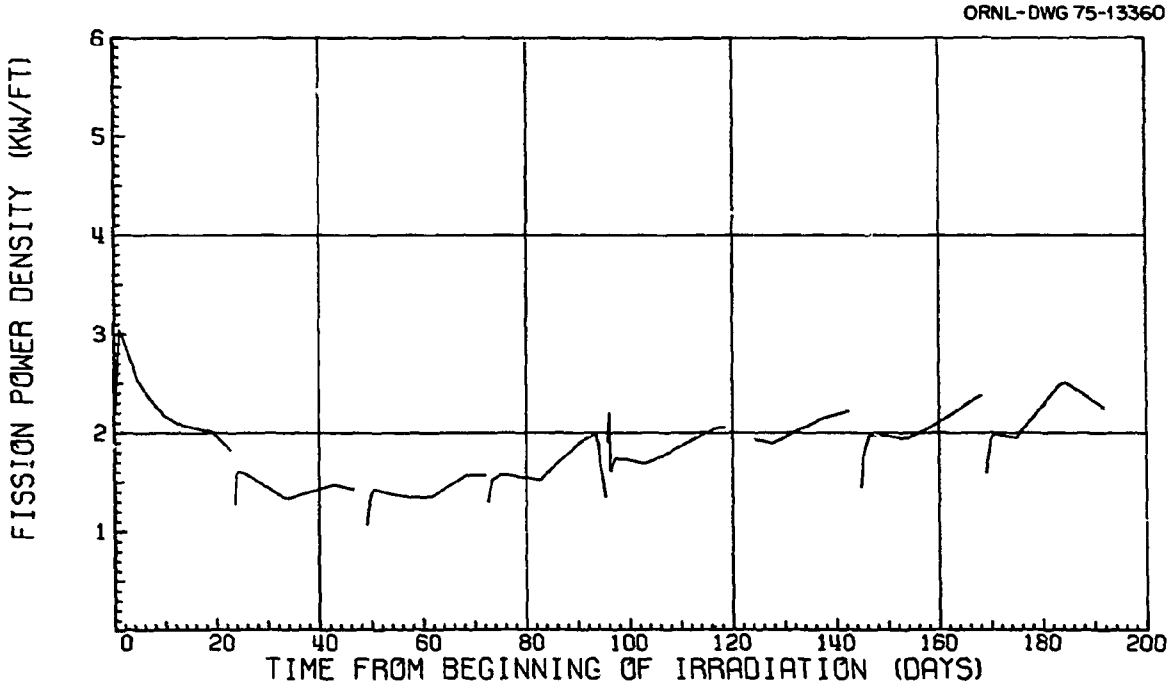

Fig. A7. Fission Heat Rate vs Time for HRB-6 at Axial Midpoint of Specimen 3D.

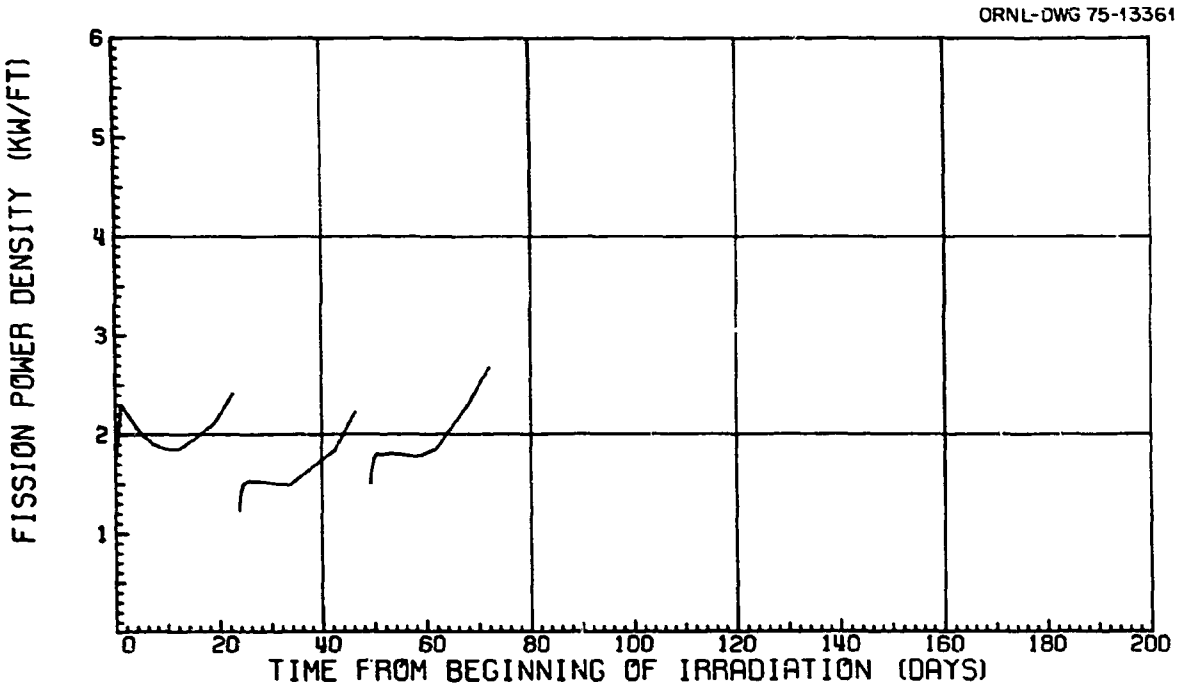

Fig. A8. Fission Heat Rate vs Time for HRB-6 at Axial Midpoint of Specimen 4B.

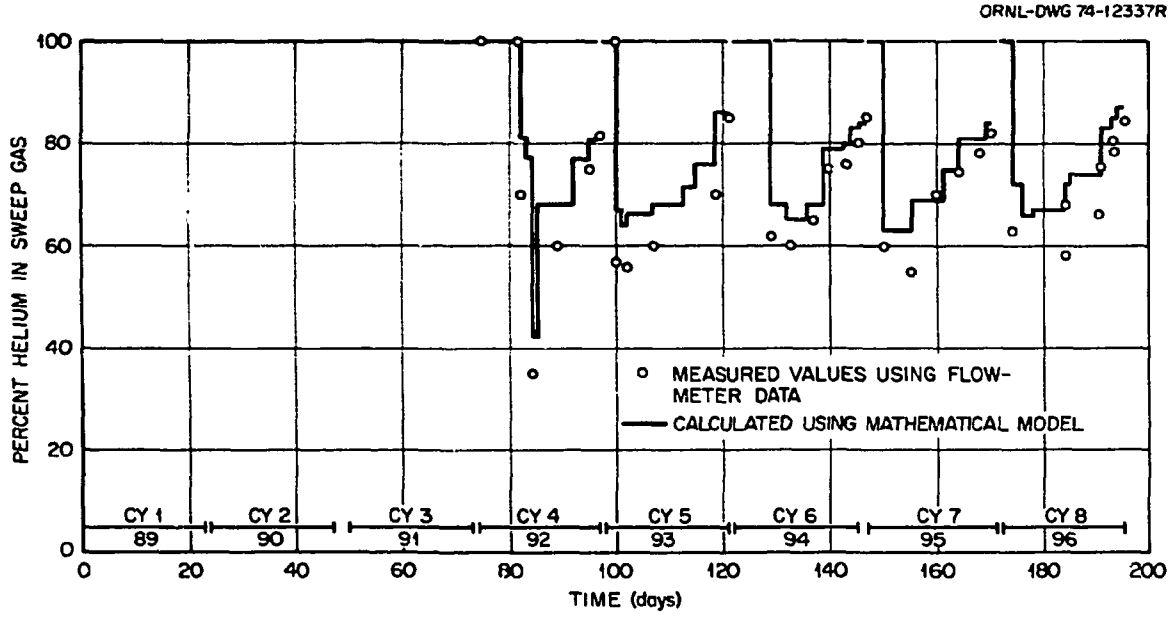

Fig. A9. Sweep Gas Composition vs Time in HRB-6.

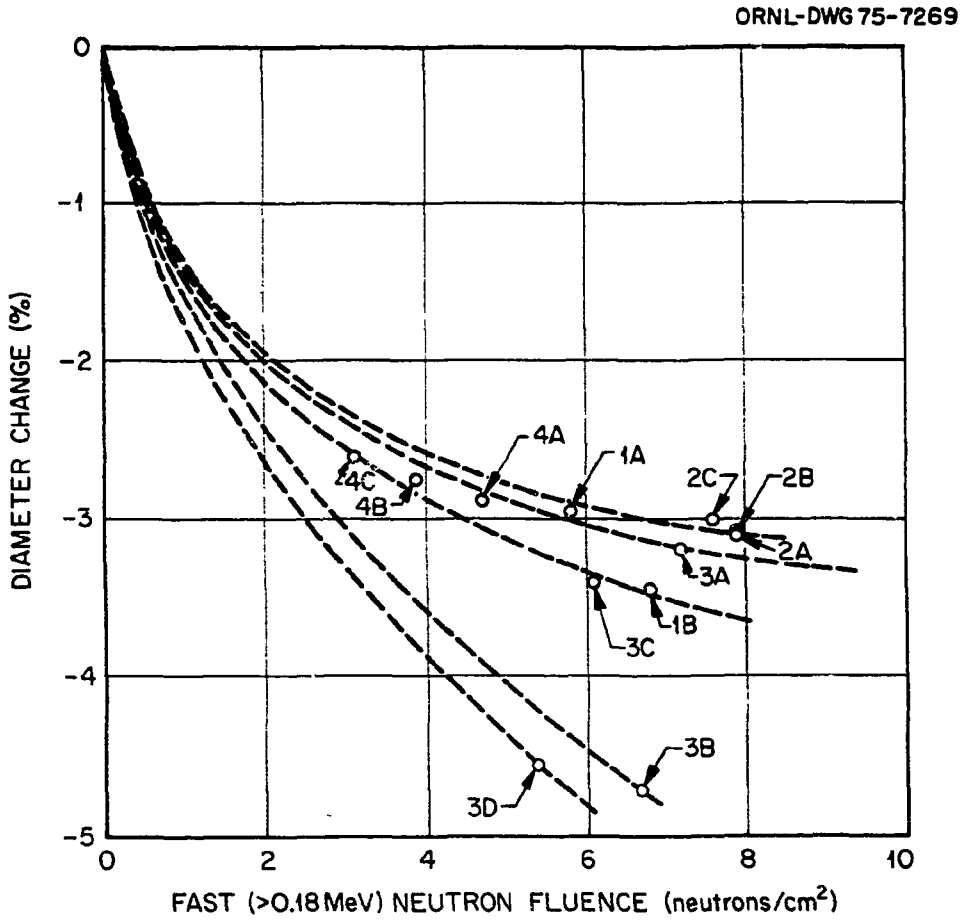

Fig. A10. Dimensional Change Data for Fuel Rods from HRB-6.

knowledge of dimensional changes derived from previous experiments.[3,5,6] Figures A11 and A12 show the preirradiation and postirradiation graphite sleeve dimensions. Graphite swelling is assumed to occur in approximately linear fashion with fast fluences.

---

[5]J. H. Coobs et al., *Irradiation Performance in HFIR Experiment HRB-2 of HTGR Fuel Sticks Bonded with Reference and Advanced Matrix Materials*, ORNL-TM-3988 (January 1973).

[6]R. B. Fitts et al., *Gas-Cooled Reactor Programs Annu. Progr. Rep. Dec. 31, 1972*, ORNL-4911, pp. 142–44.

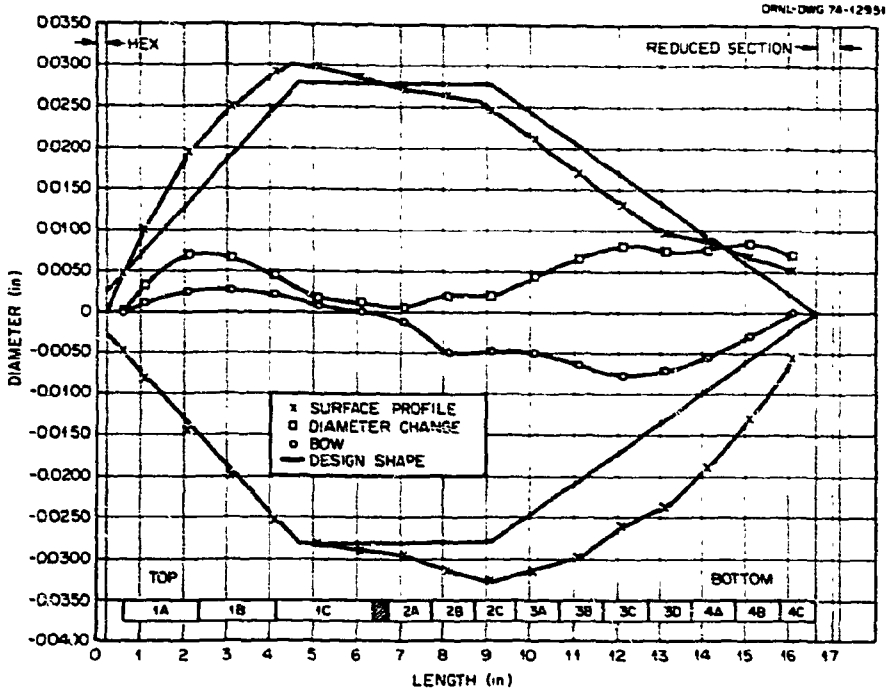

Fig. A11. Graphite Sleeve Dimensions for Capsule HRB-6 0° Orientation.

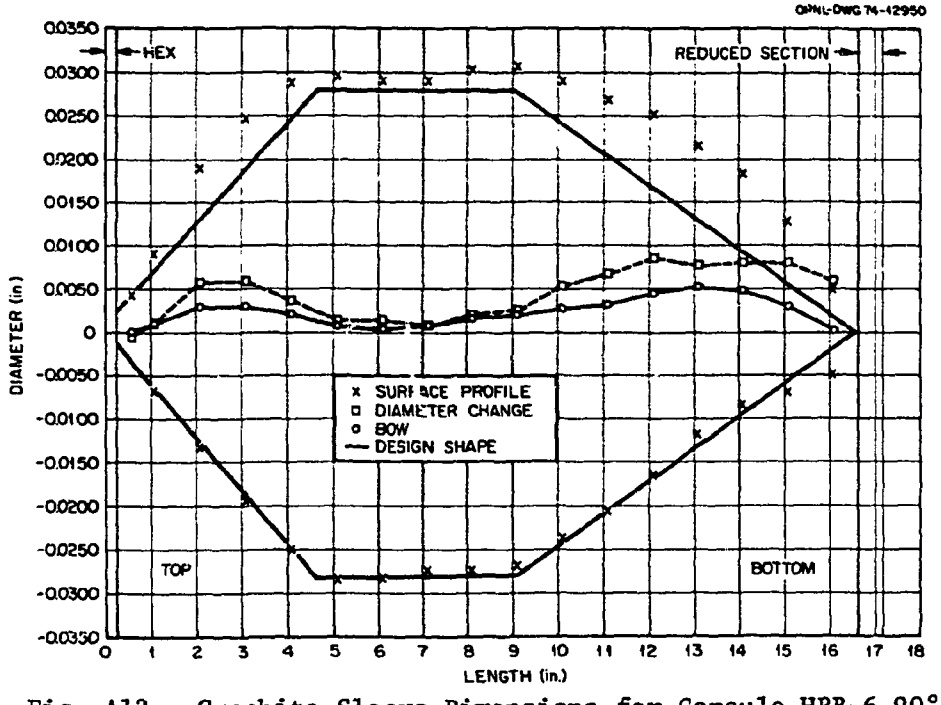

Fig. A12. Graphite Sleeve Dimensions for Capsule HRB-6 90° Orientation.

APPENDIX B

FUEL ROD MEASUREMENTS

The pre- and postirradiation dimensions of the fuel rods fabricated at ORNL and irradiated in capsule HRB-6 are shown in Table B1, as well as the percent changes in diameter and length. Note that each average diameter for a fuel rod represents six diameter measurements. The length measurement is a maximum value.

Table B1. Dimensions of Fuel Rods for HRB-6 Experiment

DIAMETERS
FROM V-BLOCK MEASUREMENTS

RADIATION EXP NO HRB-6
SPECIMEN SERIES HRB-6
POST-IRRADIATION DATA

		STANDARD	DIMENSION	GAGE
MEASURED	10-19-73	DIAMETERS	0.4902	0.1623
MEASURED	10-19-73	LENGTH	0.9803	0.1421

SPECIMEN NO		DIAMETER				LENGTH		
POSITION	GAGE	POST IRR	AVG	PRE IRR AVG	% CHANGE	PRE IRR	POST IRR	% CHANGE
3A								
00-TOP	0.1416	0.4731						
90-TOP	0.1409	0.4725	0.4728	0.4882	-3.16			
00-MID	0.1410	0.4726						
90-MID	0.1414	0.4729	0.4727	0.4880	-3.13	(GAGE 0.1115)		
00-BOT	0.1405	0.4721						
90-BOT	0.1402	0.4719	0.4720	0.4880	-3.28			
AVG		0.4725		0.4881	-3.19	0.9970	0.9497	-4.74
3B								
00-TOP	0.1344	0.4671						
90-TOP	0.1342	0.4669	0.4670	0.4903	-4.85			
00-MID	0.1344	0.4671						
90-MID	0.1332	0.4661	0.4666	0.4891	-4.60	(GAGE 0.0875)		
00-BOT	0.1334	0.4663						
90-BOT	0.1326	0.4656	0.4659	0.4889	-4.70			
AVG		0.4665		0.4896	-4.72	0.9800	0.9257	-5.54
3C								
00-TOP	0.1373	0.4695						
90-TOP	0.1377	0.4698	0.4697	0.4882	-3.80			
00-MID	0.1402	0.4719						
90-MID	0.1404	0.4721	0.4720	0.4884	-3.36	(GAGE 0.0978)		
00-BOT	0.1417	0.4731						
90-BOT	0.1430	0.4742	0.4737	0.4886	-3.06			
AVG		0.4718		0.4884	-3.41	0.9810	0.9360	-4.59
3D								
00-TOP	0.1333	0.4662						
90-TOP	0.1330	0.4659	0.4661	0.4891	-4.71			
00-MID	0.1350	0.4676						
90-MID	0.1352	0.4677	0.4677	0.4897	-4.50	(GAGE 0.0877)		
00-BOT	0.1364	0.4687						
90-BOT	0.1365	0.4688	0.4688	0.4907	-4.47			
AVG		0.4675		0.4898	-4.56	0.9720	0.9259	-4.74

Table B1. (Continued)

DIAMETERS
FROM V-BLOCK MEASUREMENTS

RADIATION EXP NO HRB-6
SPECIMEN SERIES HRB-6
POST-IRRADIATION DATA

		STANDARD	DIMENSION	GAGE
MEASURED	10-19-73	DIAMETERS	0.4900	0.1621
MEASURED	10-19-73	LENGTH	1.7500	0.1421

SPECIMEN NO

		DIAMETER				LENGTH		
POSITION	GAGE	POST IRR	AVG	PRE IRR AVG	% CHANGE	PRE IRR	POST IRR	% CHANGE
1A								
00-TOP	0.1482	0.4785						
90-TOP	0.1478	0.4782	0.4783	0.4923	-2.83			
00-MID	0.1474	0.4778						
90-MID	0.1471	0.4776	0.4777	0.4916	-2.83	(GAGE 0.0946)		
00-BOT	0.1455	0.4765						
90-BOT	0.1464	0.4770	0.4767	0.4924	-3.18			
AVG		0.4776		0.4921	-2.95	1.7690	1.7025	-3.76
1B								
00-TOP	0.1430	0.4742						
90-TOP	0.1428	0.4740	0.4741	0.4906	-3.36			
00-MID	0.1424	0.4737						
90-MID	0.1427	0.4739	0.4738	0.4910	-3.50	(GAGE 0.0912)		
00-BOT	0.1426	0.4738						
90-BOT	0.1418	0.4732	0.4735	0.4906	-3.47			
AVG		0.4738		0.4907	-3.45	1.7620	1.6991	-3.57